A FOURIER METHOD FOR IMAGE RECONSTRUCTION USING PROJECTION DATA

by

DAKSHESH D. PARIKH

B.E., M. S. University of Baroda, 1973

A MASTER'S THESIS

submitted in partial fulfillment of the

requirements for the degree

MASTER OF SCIENCE

Department of Electrical Engineering

KANSAS STATE UNIVERSITY
Manhattan, Kansas

1976

Approved by:

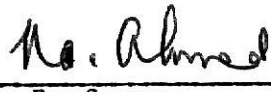

Major Professor

ACKNOWLEDGMENTS

I wish first of all to thank my parents for making it possible for me to be here to do this work. Also I wish to express my deepest thanks and appreciation to Dr. N. Ahmed who, as my advisor, suggested the topic for the thesis and who provided both guidance and encouragement during the writing of the thesis. Thanks are also due to Mr. T. Natarajan and David Hein for their help and encouragement. Additionally, I would like to thank the Department of Electrical Engineering, Kansas State University, for providing financial support. Thanks are also due to Mrs. Patricia Stewart for typing the thesis.

Finally, personal notes of gratitude go to my sister and brother-in-law, Varsha and Yogesh, without whose encouragement, patience, and understanding the work would surely have been much more difficult.

TABLE OF CONTENTS

LIST OF TABLES

LIST OF FIGURES

CHAPTER I

INTRODUCTION

The problem of reconstructing 3-dimensional objects from a set of 2-dimensional projected images is of great importance in fields ranging from medicine to radio astronomy. In all these cases one takes a series of 2-dimensional sections of the 3-dimensional object, and for each 2-dimensional section collects the ray-sum or projection for a series of non-overlapping rays. These rays are chosen such that they cover the elements or lattice points of the 2-dimensional cross-section. Then each plane is reconstructed independently of the other planes and the reconstructions for different planes are stacked to reconstruct the 3-dimensional object.

Many different reconstruction methods are available. It is possible to divide such methods into thirteen categories [2]. However, there are basically two major categories [3,4] one in which reconstruction is performed in normal signal space, and the other in which it is performed in the Fourier space. First we briefly discuss a few of the methods which perform the desired reconstruction in signal space. This is followed by a discussion pertaining to the Fourier methods.

1.1. Reconstruction in the Signal Space

(a). Direct-matrix and Linear Equation Method. Projection data at different angles is obtained, and a linear equation corresponding to each projection is written. Thus in general, this method requires one solve a set of simultaneous equations which could involve the inversion of large matrices.

For example, in the case of a 64 x 64 array, 4096 simultaneous equations must be solved, which implies that a very large matrix inversion is necessary. In addition the corresponding system of equations is invariably undetermined and inconsistent. Again, a generalized inverse formulation is sometimes used. In any case this approach is quite limited in its scope and hence not considered for implementation purposes.

(b). Linear Superposition or Back Projection. The simplest and most rapid method of reconstructing a 2-dimensional distribution from multiple 1-dimensional projections is to merely project the views back to a common object region. This technique is basically that of conventional tomography or laminography, implemented by analog methods of moving the imaging system relative to the object. The strings of data for the multiple views are superposed on film by changing the angle of display relative to the film corresponding to the change in angle of view from one scan to the next. The result is the superposition of the projections. Though this technique is very simple, the resulting reconstruction will not equal the true image because each point is formed by the superposition of a set of straight lines corresponding to each projected ray from the true object.

(c). Algebraic Reconstruction Technique (ART). Gordon [6] applied this method to the reconstruction of a 50 x 50 digitized image from computed projections. The simple algorithm consists of guessing a value for all the picture elements and then modifying each element along each ray by a factor that compensates for the discrepancy between the measured ray sum and the calculated ray sum. If the calculated ray sum is the same as the measured value, it implies that the guess values are correct for a particular

projection; however, for another projection there might be a large discrepancy. Hence the picture elements of the last view are modified according to the discrepancy between the new ray sum and the measured value. Thus each ray belonging to a given projection is examined and values of the picture elements falling within that ray are changed iteratively over five to ten iterations. This process is repeated, one projection at a time, and is called multiplicative ART. Another method of correcting the discrepancy between the measured projections consists of adding the difference between the measured ray sum and the estimated ray sum. This is called the additive form of ART.

(d) Simultaneous Iterative Reconstruction Technique (SIRT). This method was developed by Gilbert (1972a.) [7]. The SIRT method differs from ART in that in each iteration the densities of picture elements are altered by using the data from all of the projections simultaneously. The SIRT method gives results which are in close agreement with those produced by the Fourier method.

There are several other techniques which belong to the category where reconstruction is carried out in the original data space. The interested reader may refer to the pertinent references, some of which are cited at the end [8,9,10,11].

1.2. Reconstruction in the Fourier Space.

The problem of reconstructing an image in the Fourier space was introduced in 1956 by Bracewell [12]. In this approach, a theorem which is referred to as the projection slice theorem [3] plays an important role. In essence it states that the Fourier transform of a projection yields a

slice of the Fourier transform of the projected image. There are several algorithms available, such as those by DeRosier and Klug [13], Crowther, DeRosier, and Klug [14], Budinger [15], Lake [16], and Peters et al. [17].

This research effort is motivated by some of the relatively recent work of Mersereau [3, 4]. It is shown that an (N x N) noiseless, bandlimited image can be reconstructed from either a set of 3N/2 projections, or a single projection, without resorting to any tedious computational techniques. This result is in agreement with the conjecture by Mersereau which states that exact reconstruction should be possible with the number of projections is of the order of N/2 [3]. Again, the second result which is attributed to this work is also consistent with Mersereau's one projection theorem, which states that exact reconstruction is possible via only one projection. However, in this thesis it is shown that a particular projection yields projection data which corresponds to the rows of a given digital image arranged in lexicographical order [5]. As a consequence, the resulting reconstruction process requires no tedious calculations, and is equivalent to the conventional procedure for computing the 2-dimensional DFT using a 1-dimensional FFT of size N^2, where the corresponding algorithm is derived via a matrix Kronecker product formulation.

Chapter II is concerned with the developments of the above results. A computer program which enables one to generate projection data is presented in Chapter III, along with a software implementation for an algorithm called the 3N/2-reconstruction algorithm. This algorithm enables one to reconstruct a noiseless, bandlimited digital image from the projection data obtained via 3N/2 projections. The programming language used for the implementation is FORTRAN. Finally, some conclusions and suggestions for future work are presented in Chapter IV.

CHAPTER II

EXACT RECONSTRUCTION USING A FOURIER APPROACH

2.1. Introduction

A 3-dimensional object can be regarded as a stack of 2-dimensional planes. Hence the reconstruction of a 3-dimensional object can be achieved by reconstructing each of the 2-dimensional planes separately and restacking them together. Here we restrict our attention to the problem of reconstructing a 2-dimensional signals from their 1-dimensional projections. However, the corresponding formulation can be extended to the N-dimensional case.

In this chapter we show that an (NxN) noiseless bandlimited digital image can be recontructed exactly from either a set of 3N/2 projections, or a single projection, without resorting to any tedious computational techniques. In connection with the single projection case, we further show that the reconstruction process is equivalent to the conventional algorithm for computing the 2-dimensional DFT using a 1-dimensional FFT of size N , where the corresponding algorithm is derived via a matrix Kronocker product formulation.

2.2. Some Definitions

Total Mass. We assume that the cross-section of a given object can be considered as a bandlimited (NxN) digital image which can be represented by the set of discrete densities $X(m_1,m_2)$; m_1, m_2 = 0,1,2....,N-1. The coordinate system associated with it is shown in Fig. 2-1 (a). Without loss of generality, we assume that N is of the form $N=2^n$, $n=1,2,3.....n_{max}$.

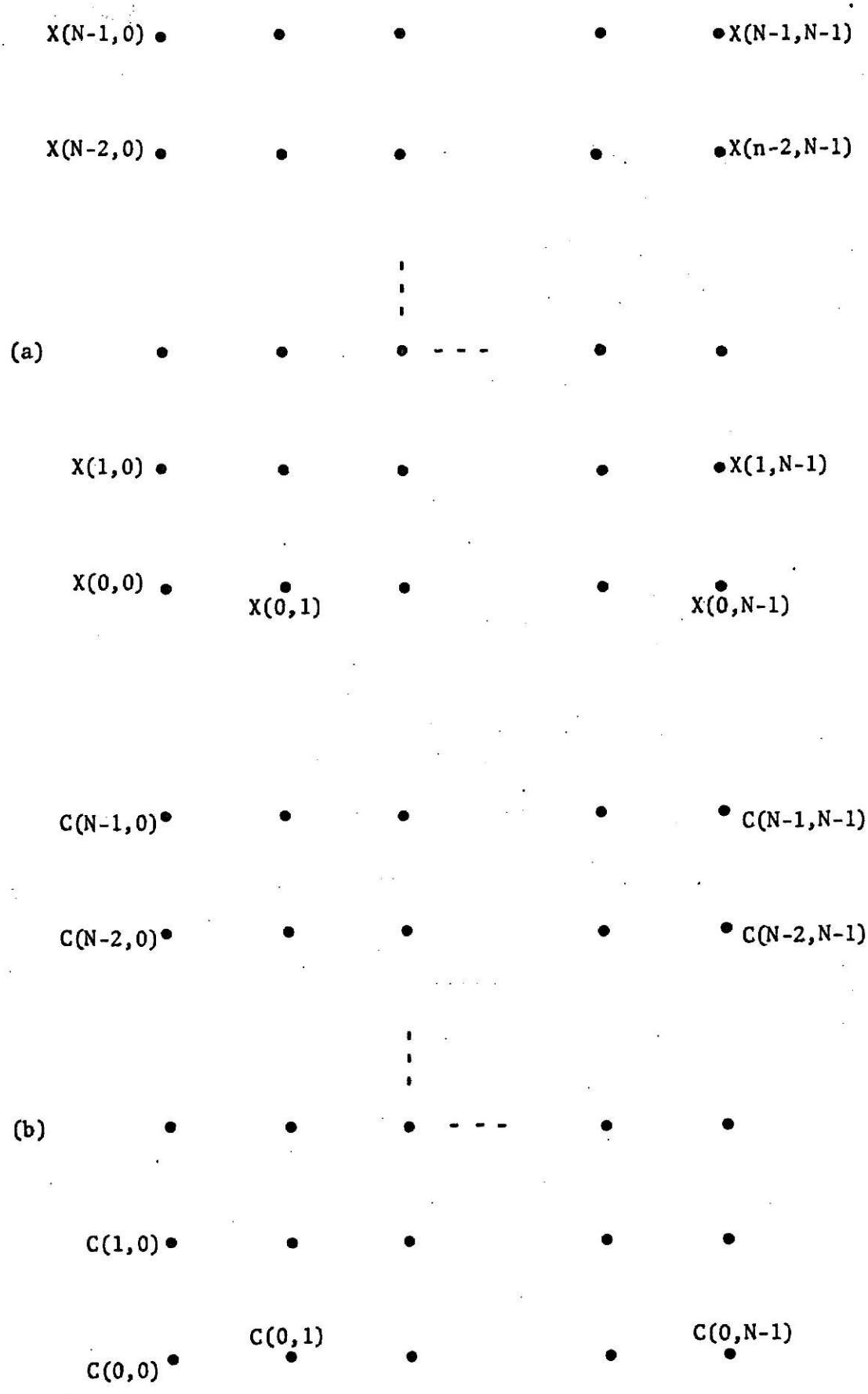

Fig.2-1. Image and Fourier coordinate systems.

Then, the total mass associated with the density is defined as

$$M = \sum_{m_1=0}^{N-1} \sum_{m_2=0}^{N-1} X(m_1,m_2) \qquad (2.2\text{-}1)$$

Bandwidth. If the distance between successive density points in Fig. 2-1(a) is denoted by Δt, then the bandwidth B of the image is given by

$$B = 1/2\,\Delta t \qquad (2.2\text{-}2)$$

Without loss of generality, it is assumed that the distance between successive density points Δt in Fig. 2-1(a) is unity.

2-Dimensional Discrete Fourier Transform. The 2-dimensional discrete Fourier transform (DFT) of the image is defined as [1]

$$C(k_1,k_2) = \frac{1}{N^2} \sum_{m_2=0}^{N-1} \sum_{m_1=0}^{N-1} X(m_1,m_2) W^{(k_1m_1+k_2m_2)};$$

$$k_1,k_2=0,1,2\ldots,(N-1). \qquad (2.2\text{-}3)$$

where $C(k_1,k_2)$ is a DFT coefficient, and $W=e^{-i2\pi/N}$. The coordinate system associated with the $C(k_1,k_2)$ is to be as shown in Fig. 2-1(b). In Eq.(3) we note that the DFT coefficients $C(k_1,k_2)$, $k_1,k_2=0,1,2,\ldots,(N-1)$ are N-periodic in both directions; i.e. with respect to the variables k_1 and k_2. This periodic property can be expressed as

$$C(N+\ell_1,\ell_2) = C(\ell_1,N+\ell_2) = C(N+\ell_1,N+\ell_2) = C(\ell_1,\ell_2);$$

$$\ell_1,\ell_2=0,1,2,\ldots,(N-1). \qquad (2.2\text{-}4)$$

2.3. Projection Considerations

A projection is defined as a mapping of a 2-dimensional function to a 1-dimensional function, where this mapping is realized by summing all the

densities along lines in a particular direction.

For example

$$P(m_1) = \sum_{m_2=0}^{N-1} X(m_1,m_2);\ m_1=0,1,\ldots,(N-1) \qquad (2.3\text{-}1)$$

denotes the projection of a 2-dimensional function $X(m_1,m_2)$ on to a line m_1 and is obtained by summing all the densities along lines in the m_2-direction, as illustrated in Fig. 2-2.

To define a projection in general, let us define a new coordinate system (u_1,u_2) which is displaced by an angle θ with respect to (x_1,x_2) as shown in Fig. 2.3(a). It follows the relation between (x_1,x_2) and (u_1,u_2) is given by

$$\begin{bmatrix} x_1 \\ \\ x_2 \end{bmatrix} = \begin{bmatrix} \cos\theta & -\sin\theta \\ \\ \sin\theta & \cos\theta \end{bmatrix} \begin{bmatrix} u_1 \\ \\ u_2 \end{bmatrix} \qquad (2.3\text{-}2)$$

where $|x_i| \leq \infty$, $|u_i| \leq \infty$, and $i = 1,2$.

Hence the relation between (m_1,m_2) and (u_1,u_2) is also given by

$$\begin{bmatrix} m_2 \\ \\ m_1 \end{bmatrix} = \begin{bmatrix} \cos\theta & -\sin\theta \\ \\ \sin\theta & \cos\theta \end{bmatrix} \begin{bmatrix} u_1 \\ \\ u_2 \end{bmatrix} , \quad m_1,m_2=0,1,2,\ldots \qquad (2.3\text{-}3)$$

where $\begin{bmatrix} \cos\theta & -\sin\theta \\ \sin\theta & \cos\theta \end{bmatrix}$ is an orthonormal matrix.

An important property of the above transformation is that a rotation of the coordinates (x_1,x_2) in the signal space by an angle θ results in the

THIS BOOK CONTAINS NUMEROUS PAGES WITH DIAGRAMS THAT ARE CROOKED COMPARED TO THE REST OF THE INFORMATION ON THE PAGE.

THIS IS AS RECEIVED FROM CUSTOMER.

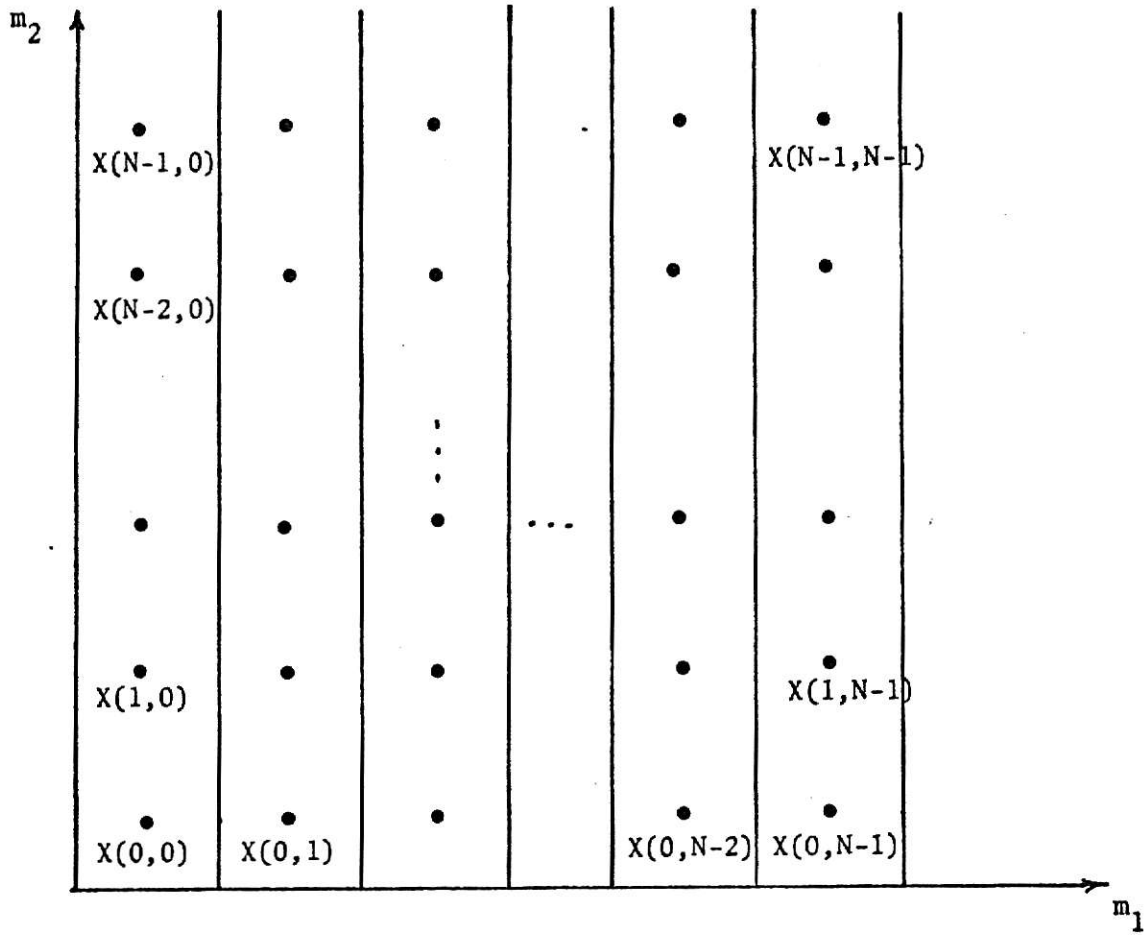

Fig. 2-2. Projection on m_1 axis.

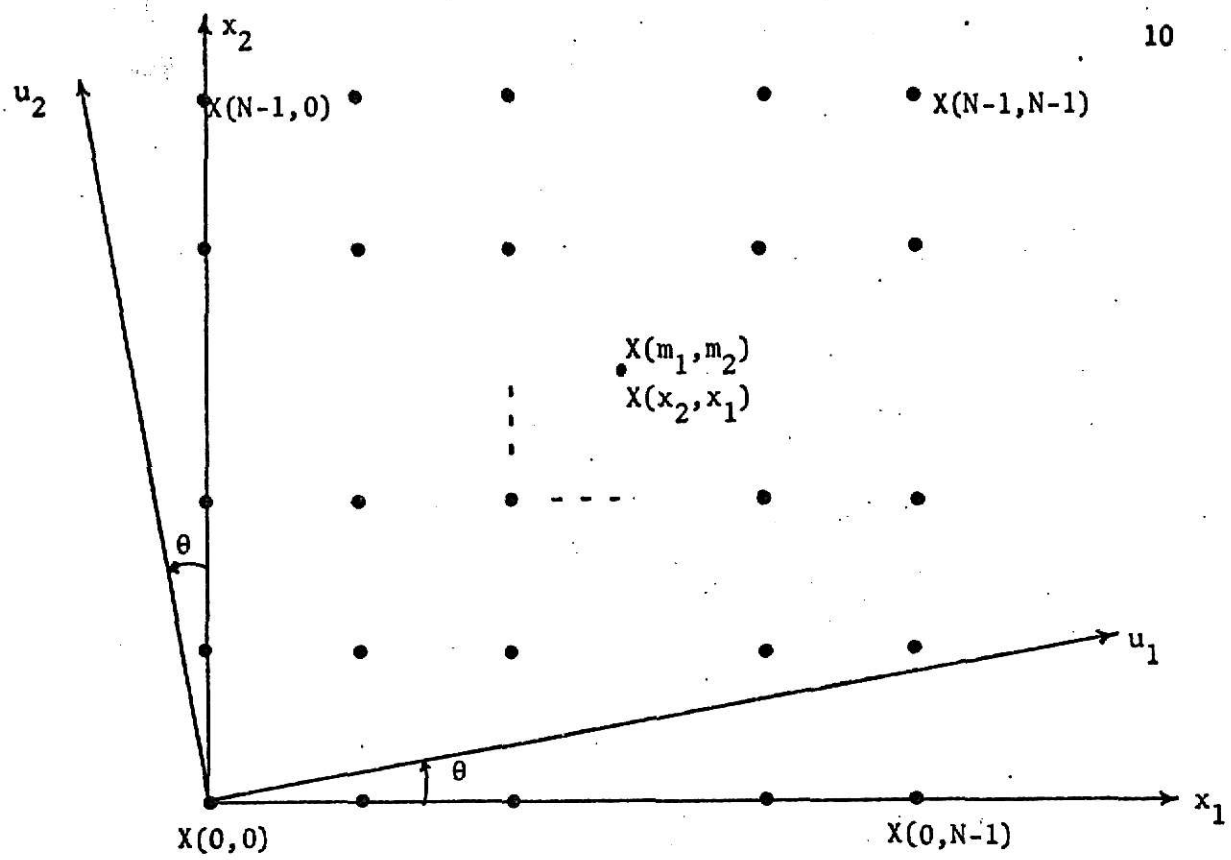

(a)

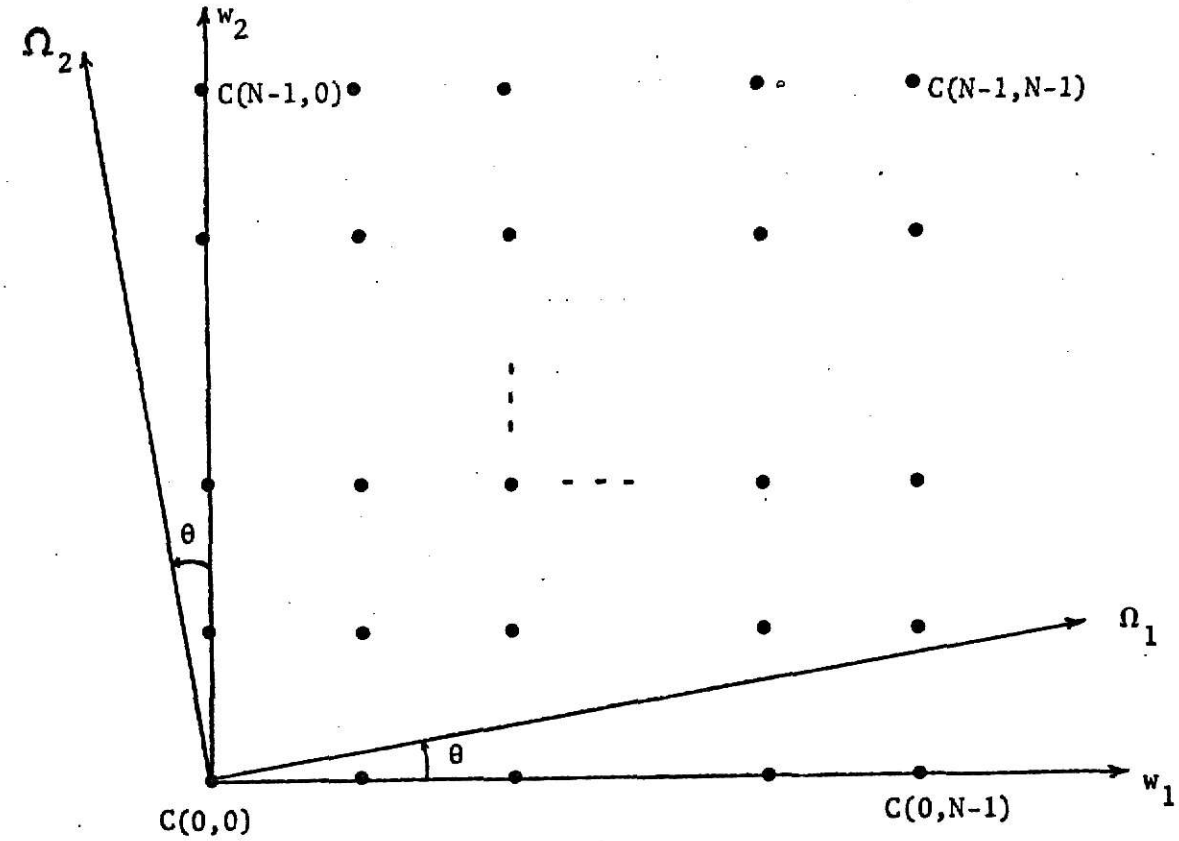

(b)

Fig. 2-3. Original and Rotated axis in signal space and Fourier space.

same rotation of the coordinates (w_1,w_2) in the Fourier space as illustrated in Fig. 2.3.

Thus in general, the projection associated with an angle θ is defined as

$$p_\theta(u_1) = \sum_{u_1} X(m_1,m_2) \qquad (2.3\text{-}4)$$

where $p_\theta(u_1)$ is the projection of the 2-dimensional function $X(m_1,m_2)$ on to the line u_1; it is obtained by summing all the densities along lines in the u_2-direction. We shall refer to u_1 as the projection axis and θ as the projection angle.

For the purposes of illustration, the projection data values $P_\theta(s)$, $s=0,1,\ldots,9$ which result from a (4x4) image for a projection angle $\theta = \tan^{-1}(1/2)$, and a particular ray width $w_\theta = 1/\sqrt{5}$ are shown in Fig. 2-4. From Fig. 2-4 it is apparent that the corresponding projection data is as follows:

$$\begin{aligned}
P(0) &= x(0,0)\\
P(1) &= x(1,0)\\
P(2) &= x(0,1) + x(2,0)\\
P(3) &= x(1,1) + x(3,0)\\
P(4) &= x(0,2) + x(2,1)\\
P(5) &= x(1,2) + x(3,1)\\
P(6) &= x(0,3) + x(2,2)\\
P(7) &= x(1,3) + x(3,2)\\
P(8) &= x(2,3)
\end{aligned}$$

and

$$P(9) = x(3,3) \qquad (2.3\text{-}5)$$

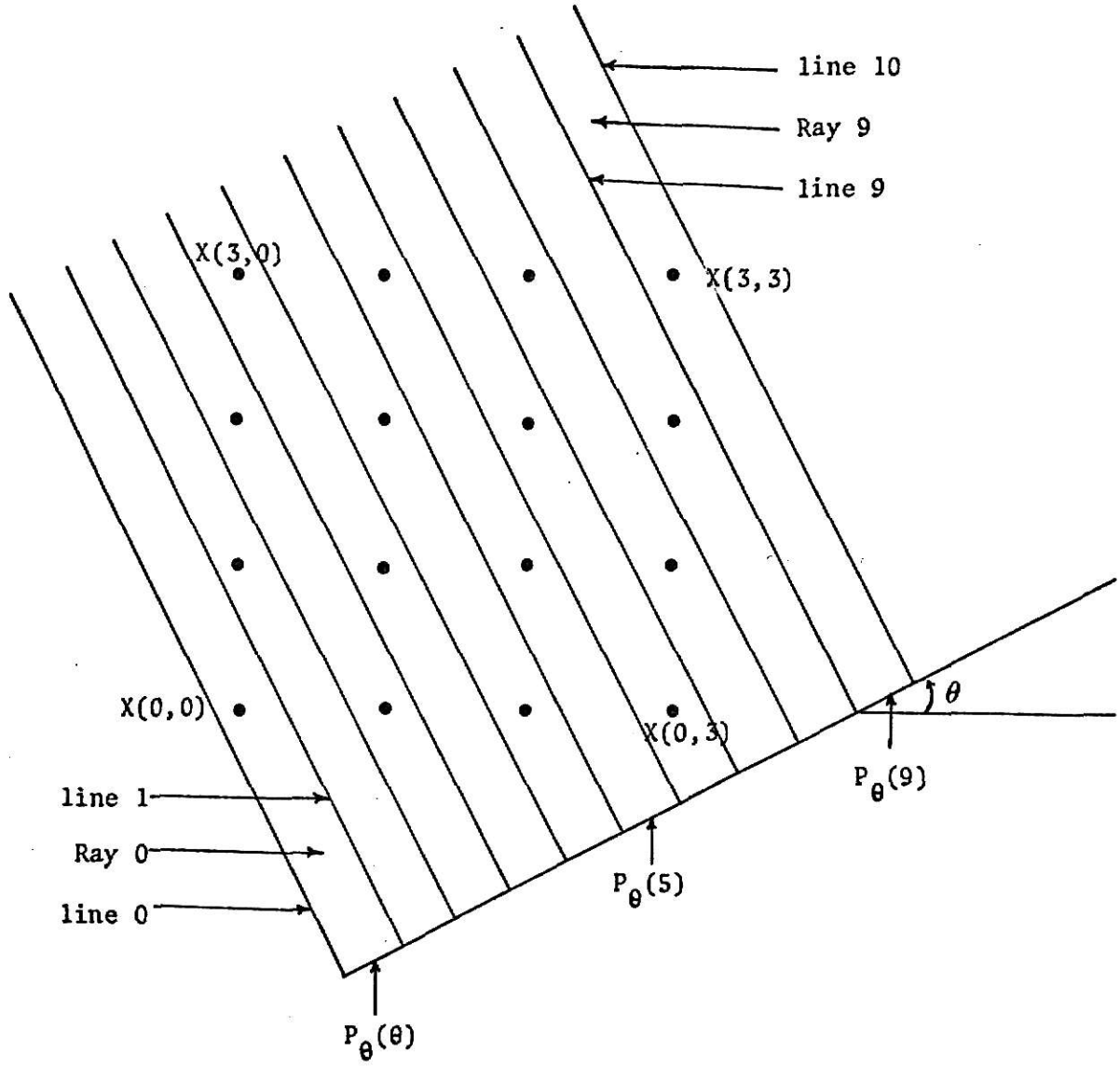

Fig. 2-4. Projection data for N = 4 and $\theta = \tan^{-1}(1/2)$

We recall that the summation along the u_1 direction gives the total mass M, since the projection on the u_1-axis is the summation of all the densities in u_2-direction. Hence Eqs. (4) and (2.2-1) yield

$$M = \sum_{u_1} p_\theta(u_1) = \sum_{m_2=0}^{N-1} \sum_{m_1=0}^{N-1} X(m_1,m_2) \tag{2.3-6}$$

2.4. A Specific Class of Projections

We now consider the specific projections, when the projection angle θ is chosen such that

$$\theta = \tan^{-1}(k_1/k_2) \tag{2.4-1}$$

where k_1 and k_2 correspond to the frequency numbers associated with the DFT coefficient $C(k_1,k_2)$ in Eq.(2.2-3). In what follows, we obtain the set of projections associated with these projection angles.

From Eq.(2.3-6) we have

$$p_\theta(u_1) = \sum_{u_2} X(m_1,m_2) \tag{2.4-2}$$

where [see Eq.(2.3-3)]

$$\begin{aligned} u_1 &= m_1 \sin\theta + m_2 \cos\theta \\ u_2 &= m_1 \cos\theta - m_2 \sin\theta \end{aligned} \tag{2.4-3}$$

or

$$\begin{aligned} m_1 &= u_1 \sin\theta + u_2 \cos\theta \\ m_2 &= u_1 \cos\theta - u_2 \sin\theta \end{aligned} \tag{2.4-4}$$

Substitution of Eq.(4) in Eq.(2) leads to

$$p_\theta(u_1) = \sum_{u_2} X(u_1\sin\theta+u_2\cos\theta,\ u_1\cos\theta-u_2\sin\theta) \tag{2.4-5}$$

It is important to note that Eq.(5) is valid for any θ. Now, if θ is specifically chosen as in Eq.(1), the projection angle θ satisfies the following relations:

$$\sin\theta = k_1/\sqrt{k_1^2 + k_2^2}$$

$$\cos\theta = k_2/\sqrt{k_1^2 + k_2^2} \qquad (2.4\text{-}6)$$

From Eqs.(3) and (6) we obtain

$$u_1 = (m_1k_1+m_2k_2)/\sqrt{k_1^2 + k_2^2} = sT_\theta$$

$$u_2 = (m_1k_2-m_2k_1)/\sqrt{k_1^2 + k_2^2} = rT_\theta \qquad (2.4\text{-}7)$$

where

$$s = k_1m_1+k_2m_2$$

$$r = m_1k_2-m_2k_1 \qquad (2.4\text{-}8)$$

and

$T_\theta = 1/\sqrt{k_1^2 + k_2^2}$ is the sampling interval for the continuous projection data obtained at an angle θ.

Substituting the value of u_1, u_2, $\cos\theta$ and $\sin\theta$ from Eq.(7) and (6) in Eq.(5), we obtain

$$P_\theta(s) = p_\theta(sT_\theta) = \sum_r X([sk_1+rk_2]T_\theta^2, [sk_2-rk_1]T_\theta^2) \qquad (2.4\text{-}9)$$

Next, we determine the limits of s and r. From Fig. 2-5 it follows that u_1(or s, see Eq.(7)) attains its minimum and maximum values when

$$m_1 = m_2 = 0$$

and

$$m_1 = m_2 = (N-1)$$

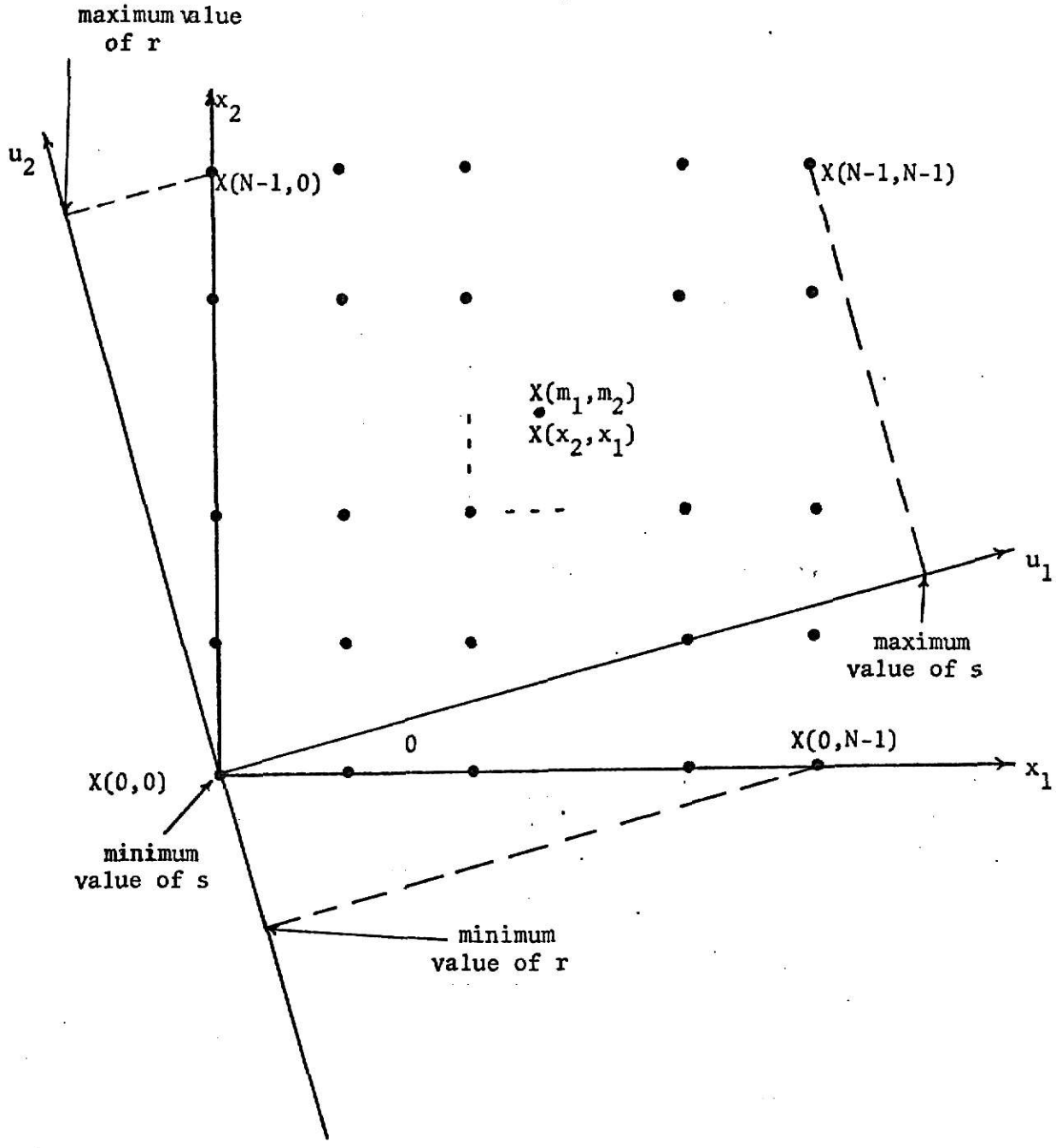

Fig. 2-5. Related to maximum and minimum values of s and r.

respectively. Again, u_2 (or r, see Eq.(7)) attains its minimum and maximum when

$$m_1 = 0,\ m_2 = (N-1)$$

and

$$m_1 = (N-1),\ m_2 = 0$$

respectively, Thus from the values of m_1 and m_2 and Eq.(8), it follows that

$$0 \le s \le (k_1+k_2)(N-1)$$

and

$$-(N-1)k_1 \le r \le (N-1)k_2 \qquad (2.4\text{-}10)$$

Using Eq.(10) we rewrite the Eq.(9) as

$$P_\theta(s) = \sum_{r=-(N-1)k_1}^{(N-1)k_2} X([sk_1+rk_2]T_\theta^2,\ [sk_2-rk_1]T_\theta^2),\ s=0,1,2,\ldots,(N_\theta-1). \qquad (2.4\text{-}11)$$

where

$$N_\theta = (N-1)(k_1+k_2)+1 \qquad (2.4\text{-}12)$$

Also using the Eq.(7), we express the Eq.(2.3-6) as

$$M = \sum_s p_\theta(sT_\theta) = \sum_{m_2=0}^{N-1} \sum_{m_1=0}^{N-1} X(m_1,m_2) \qquad (2.4\text{-}13)$$

From Eqs.(10), (12) and (13) we obtain

$$M = \sum_{s=0}^{(N_\theta-1)} P_\theta(s) = \sum_{m_2=0}^{N-1} \sum_{m_1=0}^{N-1} X(m_1,m_2) \qquad (2.4\text{-}14)$$

2.5. Fourier Transform Reconstruction

Taking the Fourier transform F_θ of $P_\theta(s)$ in Eq.(2.4-11) we obtain

$$F_\theta(\Omega_1) = T_\theta \sum_{s=0}^{N_\theta-1} P_\theta(s) e^{-i\Omega_1 sT_\theta} \qquad (2.5\text{-}1)$$

We now compute F_θ at the frequency Ω_L, where

$$\Omega_L = \frac{2\pi L}{T_\theta N} \tag{2.5-2}$$

Then Eq.(1) yields

$$F_\theta(\Omega_L) = T_\theta \sum_{s=0}^{N_\theta-1} P_\theta(s)\, e^{-i2\pi Ls/N} \tag{2.5-3}$$

From the relation of Fourier transform and DFT it follows that [1]

$$C_\theta(L) = \left(\frac{1}{N_\theta T_\theta}\right) F_\theta(\Omega_L);\ L=0,2,\ldots,(N-1). \tag{2.5-4}$$

where $C_\theta(L)$ is the L-th DFT coefficient. Combining Eqs.(3) and (4), we obtain

$$C_\theta(L) = \frac{1}{N_\theta} \sum_{s=0}^{N_\theta-1} P_\theta(s)\, W^{Ls};\ L=0,1,2,\ldots,(N-1). \tag{2.5-5}$$

where $W=e^{-i2\pi/N}$. In Eq.(5), it is observed that the $C_\theta(L)$ can be computed using the fast Fourier transform (FFT). Using the value of s from Eq.(2.4-8) we rewrite the Eq.(5) as

$$C_\theta(L) = \frac{1}{N_\theta} \sum_{s=0}^{N_\theta-1} P_\theta(s) W^{L(k_1m_1+k_2m_2)};\ L=0,1,2,\ldots,(N-1) \tag{2.5-6}$$

Combining Eqs.(2.4-14) and (6) we obtain

$$C_\theta(L) = \frac{1}{N_\theta} \sum_{m_2=0}^{N-1} \sum_{m_1=0}^{N-1} X(m_1,m_2) W^{L(k_1m_1+k_2m_2)};\ L=0,1,2,\ldots,(N-1) \tag{2.5-7}$$

A comparison of Eqs.(7) and (2.2-3) leads to the following important result:

$$C(Lk_1,Lk_2) = (N_\theta/N^2)C_\theta(L),\ L=0,1,2,\ldots,(N-1) \tag{2.5-8}$$

If the scale factor (N_θ/N^2) in Eq.(8) is ignored, then it can be written as

$$C(Lk_1,Lk_2) = C_\theta(L),\ L=0,1,2,\ldots,(N-1) \qquad (2.5\text{-}9)$$

From Eq.(9) it can be seen that the projection data associated with (k_1,k_2) yields N 2-dimensional DFT coefficients. This is because of its doubly periodic property with respect to k_1 and k_2, i.e. for a given (k_1,k_2) we obtain the set of indices (ℓ_1,ℓ_2) which satisfies the congruence

$$\{(\ell_1,\ell_2)\} = \{Lk_1(\text{mod } N),\ Lk_2(\text{mod } N)\},\ L=0,1,2,\ldots,(N-1)$$
$$0 \le \ell_1,\ell_2 \le (N-1) \qquad (2.5\text{-}10)$$

We remark that Eqs.(10) and (2.2-4) represent the same property. For example with N=4, k_1=1, and k_2=2, Eq.(9) yields

$$C(L,2L) = C_\theta(L),\ L=0,1,2,3. \qquad (2.5\text{-}11)$$

Again, from Eqs.(11) and (10) we obtain

$$C_\theta(0) = C(0,0)$$
$$C_\theta(1) = C(1,2)$$
$$C_\theta(2) = C(2,4) = C(2,0)$$
$$C_\theta(3) = C(3,6) = C(3,2) \qquad (2.5\text{-}12)$$

Hence we conclude that if the proper set of grid points $\{(k_1,k_2)\}$ are chosen, then all the desired 2-dimensional DFT coefficients can be computed via Eqs. (8) and (10).

2.6. Critical Grid Points

Consider the set of all possible grid point. It is given by

$$S = \{(0,0),\ (0,1),\ (1,0),\ (1,1),\ldots\ldots,(N-1,N-1)\}$$

We seek a subset of S which is denoted by S*. This subset is such that its elements satisfy two properties which are as follows:

(i) If $(k_1,k_2)^* \in S^*$, then k_1 and k_2 are such that they are relatively prime to one another.

(ii) If $(k_1^i, k_2^i)^*$ and $(K_1^j,k_2^j)^*$ are two elements of S^*, then they satisfy the condition

$$(K_1^j,k_2^j) \neq (nk_1^i+r_1N,\ nk_2^i+r_2N),\ n=2,3,\ldots,(N-1) \qquad (2.6\text{-}1)$$

for <u>all</u> integer values of r_1 and r_2.

To illustrate, we consider the case when $(k_1,k_2)^* = (1,3)$, $n=3$, $r_1=0$ and $r_2=-2$, then we have

$$(nk_1+r_1N,\ nk_2+r_2N) = (3x1+4x0,\ 3x3-4x2) = (3,1) \qquad (2.6\text{-}2)$$

Hence from Eq.(2) it is clear that if $(1,3) \in S^*$, than $(3,1)$ can not belong to S^*. It is important to note that the overall effect of the property in Eq.(1) is that it eliminates grid points whose related projection data yield <u>identical</u> set of 2-dimensional DFT coefficients. To illustrate, we consider $N=4$ and $(k_1,k_2) = (1,3)$. Then, from Eq.(2.5-10) it follows that the set of indices (ℓ_1,ℓ_2) associated with the 2-dimensional coefficients $C(\ell_1,\ell_2)$ are as follows:

$$\left\{(\ell_1,\ell_2)\right\}_{1,3} = \left\{(0,0),\ (1,3),\ (2,2),\ (3,1)\right\} \qquad (2.6\text{-}3)$$

Again, with $(k_1,k_2) = (3,1)$, Eq.(2.5-10) yields

$$\left\{(\ell_1,\ell_2)\right\}_{3,1} = \left\{(0,0),\ (3,1),\ (2,2),\ (1,3)\right\} \qquad (2.6\text{-}4)$$

Inspection of Eqs.(3) and (4) leads to the conclusion that $\left\{(\ell_1,\ell_2)\right\}_{1,3} = \left\{(\ell_1,\ell_2)\right\}_{3,1}$. In other words, the projection data associated with the projection angles $\theta_1 = \tan^{-1}(1/3)$ and $\theta_2 = \tan^{-1}(3/1)$ yield the same set

of 2-dimensional DFT coefficients. Hence it suffices to include only one of these grid points in the set S*. In what follows, we refer to S* as the critical set. Again, each grid point $(k_1,k_2)^*$ belonging to S* will be referred to as a critical grid point.

We remark that there exist a more than one critical set. It is straightforward to verify that the following set of grid points satisfy the requirements of critical grid points, and hence constitute a critical set.

$$k_1 = 1,\ k_2 = m,\ m=0,1,2,\ldots,(N-1)$$

and

$$k_2 = 1,\ k_1 = 2n,\ n=0,1,2,\ldots,(\frac{N}{2} - 1) \qquad (2.6\text{-}5)$$

The critical grid points obtained via Eq.(5) for the case N=8 are shown in Fig. 2-6, and denoted by "*". Equation (5) implies that there are 3N/2 critical grid points in the critical set. This is true in general, since any other critical set can be obtained merely by replacing one or more elements of the above critical set via the congruence relation [see Eq.(2)]

$$(\alpha, \beta) = (nk_1+r_1N, nk_2+r_2N),\ n=2,3,4,\ldots,(N-1). \qquad (2.6\text{-}6)$$

for all integer values of r_1 and r_2.

For example, consider N=4. Then the critical set obtained using Eq.(5) is as follows:

$$S_1^* = \{ (1,0),\ (1,1),\ (1,2),\ (1,3),\ (0,1),\ (2,1) \} \qquad (2.6\text{-}7)$$

Now, if we consider the critical grid point (1,3), then with n = 3, $r_1 = 0$ and $r_2 = -2$, Eq.(6) yields (3,1). Hence an alternate critical set can be obtained by replacing the element (1,3) by the element (3,1); i.e.

$$S_2^* = \{ (1,0),\ (1,1),\ (1,2),\ (3,1),\ (0,1),\ (2,1) \} \qquad (2.6\text{-}8)$$

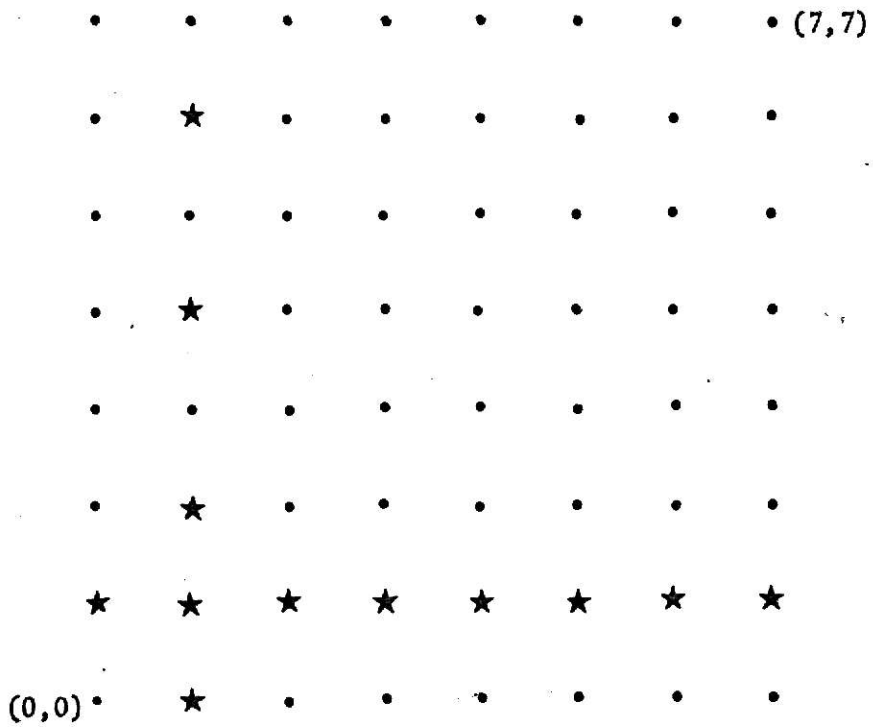

Fig. 2-6. Critical Grid points for N = 8.

For the purposes of illustration we consider N = 8. Then, the angles $\theta = \tan^{-1}(k_1/k_2)$ associated with the critical grid points given by Eq.(5) and the corresponding $C(k_1,k_2)$ given by Eqs.(2.5-9) and (2.5-10) using the pertinent projection data are as shown in Table 2.1. We remark that the 2-dimensional DFT coefficients so obtained yield the desired image points $X(m_1,m_2)$, $m_1,m_2 = 0,1,\ldots,(N-1)$ by means of the 2-dimensional inverse DFT.

2.7. The 3N/2-Reconstruction Algorithm

We are now in a position to describe an exact reconstruction algorithm. The various steps involved in this algorithm are best summarized by considering the case N = 8. In this case the desired (8x8) image can be reconstructed as follows.

Step 1: Obtain projection data corresponding to the set of critical grid points [see Fig. 2-6]

$$\left\{\begin{matrix}(1,0),\ (1,1),\ (1,2),\ (1,3),\ (1,4),\ (1,5)\\ (1,6),\ (1,7),\ (0,1),\ (2,1),\ (4,1),\ (6,1)\end{matrix}\right\} \qquad (2.7\text{-}1)$$

Step 2: For the set of 3N/2 sequences obtained in step 1, compute 1-dimensional DFT using the FFT for each sequence.

Step 3: Obtain the N^2 2-dimensional DFT coefficients from step 2 (see Table 2-1) using Eqs.(2.5-8) and (2.5-10).

Step 4: Compute the 2-dimensional inverse DFT of the N^2 2-DFT coefficients obtained in step 3. This results in to the exact image represented by $X(m_1,m_2)$, $m_1,m_2=0,1,2,\ldots,(N-1)$.

In what follows, we refer to this algorithm as the 3N/2-Reconstruction Algorithm.

From the above discussion it follows that the 3N/2-Reconstruction Algorithm conveniently yields all the N^2 2-dimensional DFT coefficients

TABLE 2.1

Coefficients obtained using projection data associated with critical angles for N=8

θ ↓	→ $C(k_1, k_2)$							
0	C(0,0)	C(0,1)	C(0,2)	C(0,3)	C(0,4)	C(0,5)	C(0,6)	C(0,7)
8.13	C(0,0)	C(1,7)	C(2,6)	C(3,5)	C(4,4)	C(5,3)	C(6,2)	C(7,1)
9.46	C(0,0)	C(1,6)	C(2,4)	C(3,2)	C(4,0)	C(5,6)	C(6,4)	C(7,2)
11.31	C(0,0)	C(1,5)	C(2,2)	C(3,7)	C(4,4)	C(5,1)	C(6,6)	C(7,3)
14.04	C(0,0)	C(1,4)	C(2,0)	C(3,4)	C(4,0)	C(5,4)	C(6,0)	C(7,4)
18.43	C(0,0)	C(1,3)	C(2,6)	C(3,1)	C(4,4)	C(5,7)	C(6,2)	C(7,5)
26.57	C(0,0)	C(1,2)	C(2,4)	C(3,6)	C(4,0)	C(5,2)	C(6,4)	C(7,6)
45	C(0,0)	C(1,1)	C(2,2)	C(3,3)	C(4,4)	C(5,5)	C(6,6)	C(7,7)
63.43	C(0,0)	C(2,1)	C(4,2)	C(6,3)	C(0,4)	C(2,5)	C(4,6)	C(6,7)
75.96	C(0,0)	C(4,1)	C(0,2)	C(4,3)	C(0,4)	C(4,5)	C(0,6)	C(4,7)
80.54	C(0,0)	C(6,1)	C(4,2)	C(2,3)	C(0,4)	C(6,5)	C(4,6)	C(2,7)
90	C(0,0)	C(1,0)	C(2,0)	C(3,0)	C(4,0)	C(5,0)	C(6,0)	C(7,0)

$C(k_1,k_2)$, $k_1,k_2 = 0,1,\ldots,(N-1)$, and a subsequent 2-dimensional inverse FFT yields the desired digital image.

2.8. Exact Reconstruction Using Only One Projection

The projection P_θ obtained at an angle $\theta = \tan^{-1}(N)$ is merely the sequence obtained by concatenating the rows of the array $[X(m_1,m_2)]$ [5]. The projection vector P_θ for this angle can also be expressed by a mapping, which is given by [3,5]

$$P_\theta(s) = P_\theta(Nm_1+m_2) = X(m_1,m_2),\ m_1,m_2=0,1,\ldots,(N-1).$$
$$s=0,1,2,\ldots,(N^2-1). \quad (2.8\text{-}1)$$

At this point we remark that this sequence is equivalent to a vector obtained by arranging the elements of the array $X(m_1,m_2)$, $m_1,m_2=0,1,\ldots,(N-1)$ in a lexicographical order [18]. For example, when $N = 4$, the projection data corresponding to $\theta = \tan^{-1}(4)$ is as shown in Fig. 2-7, and the corresponding projection vector P_θ is as follows:

$$P_\theta = \begin{bmatrix} X(0,0) \\ \vdots \\ X(0,3) \\ X(1,0) \\ \vdots \\ X(1,3) \\ X(2,0) \\ \vdots \\ X(2,3) \\ X(3,0) \\ \vdots \\ X(3,3) \end{bmatrix} \begin{matrix} \left.\begin{matrix}\\ \\ \\ \\ \end{matrix}\right\} \text{row \#1} \\ \left.\begin{matrix}\\ \\ \\ \\ \end{matrix}\right\} \text{row \#2} \\ \left.\begin{matrix}\\ \\ \\ \\ \end{matrix}\right\} \text{row \#3} \\ \left.\begin{matrix}\\ \\ \\ \\ \end{matrix}\right\} \text{row \#4} \end{matrix} \quad 16\text{x}1 \qquad (2.8\text{-}2)$$

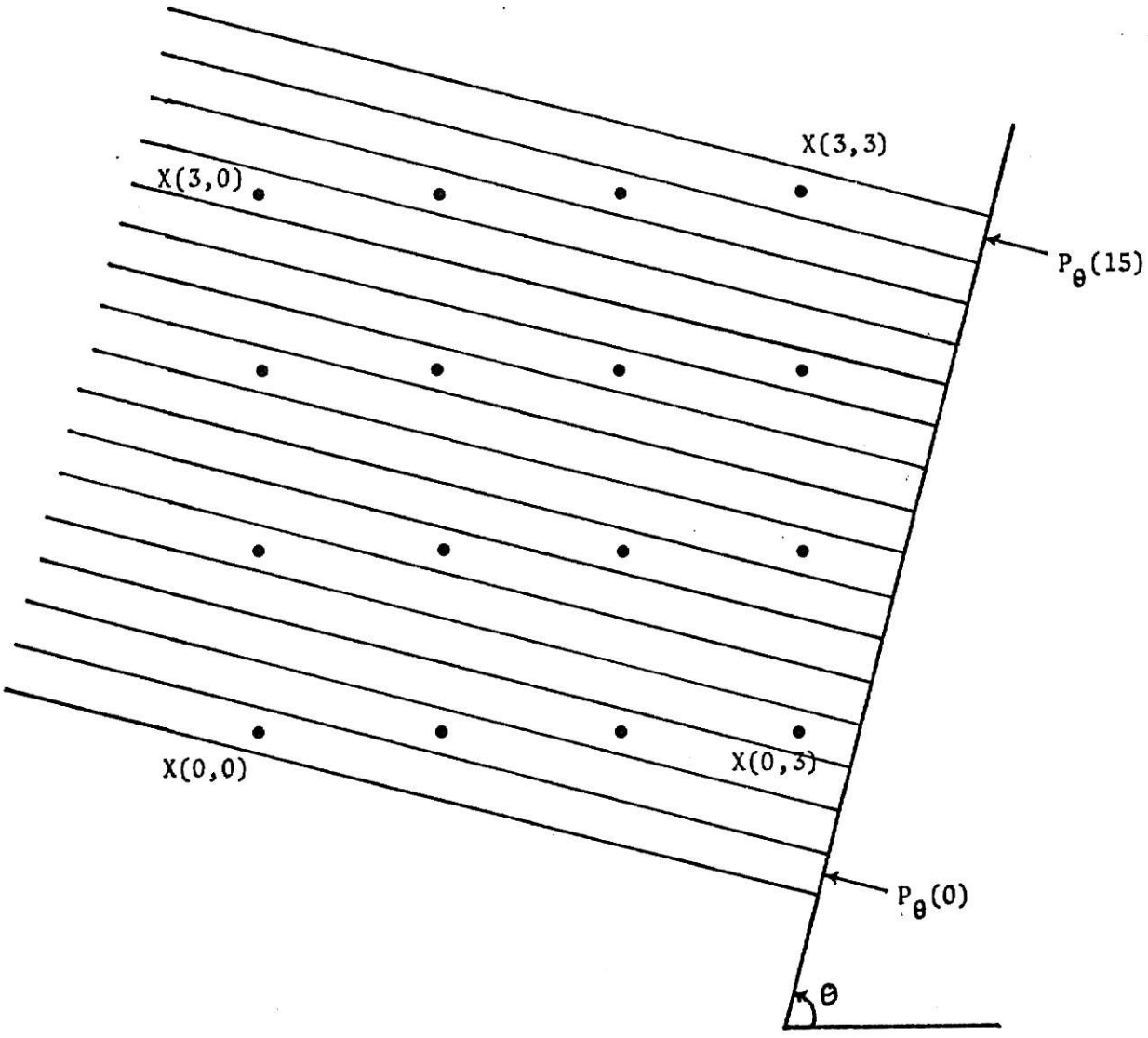

Fig. 2-7. Projection data for N = 4 and $\theta = \tan^{-1}(4)$

Now, the 2-dimensional DFT of an array $X(m_1,m_2)$, $m_1,m_2=0,1,\ldots,(N-1)$ is defined in general as [1].

$$\underline{Y} = \underline{A}\,\underline{X}\,\underline{A}' \qquad (2.8\text{-}3)$$

where $\underline{X}$ is the array $X(m_1,m_2)$, $m_1,m_2=0,1,\ldots,(N-1)$, $\underline{A}$ is the (NxN) DFT matrix, and $\underline{Y}$ is the corresponding (NxN) transform matrix. Since the projection vector P_θ corresponding to $\theta = \tan^{-1}(N)$ is the vector obtained by arranging the elements of the array $X(m_1,m_2)$, $m_1,m_2=0,1,\ldots,(N-1)$ in a lexicographical order, the 2-dimensional DFT of an array $\underline{X}$ defined in Eq.(3) is given by [18]

$$F = (\underline{A} \otimes \underline{A})\, P_\theta \qquad (2.8\text{-}4)$$

where P_θ is the N^2-projection vector at an angle $\theta = \tan^{-1}(N)$, F is the N^2-transform vector whose elements correspond to those of $\underline{Y}$ arranged in lexicographical order, and the symbol $\otimes$ denotes Kronecker product.

It can be shown that F in Eq.(4) can be computed using 2N applications of a 1-dimensional FFT of size N.

The above discussion implies that exact reconstruction is possible via projection data obtained from a single projection. This result is consistent with Mersereau's one projection theorem [3]. However, for the particular projection considered here (i.e. $\theta = \tan^{-1}(N)$), no tedious computations involving equations in polynomial form are necessary.

CHAPTER III

PROJECTION DATA SIMULATION AND ALGORITHM IMPLEMENTATION

3.1. Introduction

This chapter is concerned with details pertaining to the implementation of the 3N/2-reconstruction algorithm. The projection data at an angle θ is obtained by passing a beam of parallel rays through the cross-section of the object. An important point to observe here is that the beam of rays is not perpendicular to the cross-section as it is in the case of conventional X-ray procedures, but it is parallel to the cross-section of the object. The ray of a projection at angle θ is defined as a band of width W_θ across the plane at that angle, as shown in Fig. 3.1. The intensity of each ray is attenuated by a factor dependent upon the total densities along the ray. In practice, the intensity of the transmitted radiation is recorded by some device, typically a photographic plate. The difference in intensity, measured before and after passing through the object, gives the attenuation of the ray. The measured value of this attenuation gives the projection. The attenuation of the k-th ray depends upon the total densities $X(m_1, m_2)$ contained within the k-th ray of the projection at an angle θ as illustrated in Fig. 3.1. The total densities contained within the ray depends upon the width of the ray. Also the number of rays R_θ in a projection at angle θ depends on the width of the ray and the size of the cross-section which is to be reconstructed.

3.2. Algorithm Parameters

Ray Width. The width of the ray W_θ is not constant, but it is a function of

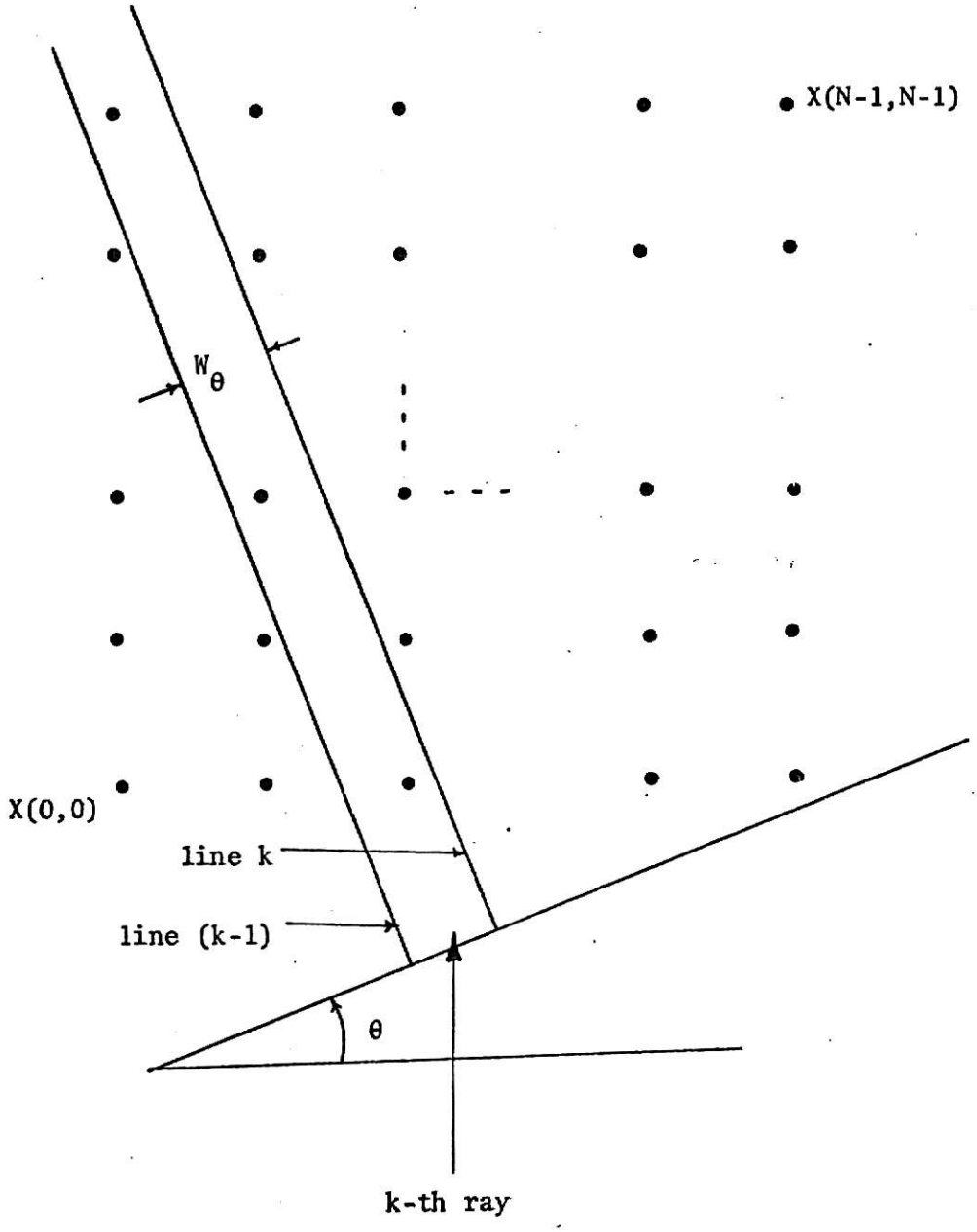

Fig. 3-1. A k-th ray having a width W_θ.

angle θ and frequency. Hence W_θ is different for each θ. Now, the ray width W_θ is merely a sampling interval T_θ which was defined in Eq. (2.4-7). Thus the ray width W_θ is given by

$$W_\theta = 1/\sqrt{k_1^2 + k_2^2} \qquad (3.2\text{-}1)$$

where θ is the projection angle and (k_1,k_2) is the critical grid point associated with projection angle θ.

Number of Rays. It is obvious that the number of rays for the projection at angle θ is merely equal to the number of elements N_θ contained in the projection vector $P_\theta(s)$ which is defined in Eq. (2.4-12). As a consequence, the number of rays R_θ at an angle θ is given by

$$R_\theta = (k_1 + k_2)(N-1)+1 \qquad (3.2\text{-}2)$$

Line Equations. We remark that each ray is considered to be the spacing between two lines of radiation as illustrated in Fig. 3-2. From Fig. 3-2, it follows that for a specified θ, the equations to the line are as follows:

$$x_1^{\ell} = (\ell - 0.5); \text{ for } \theta=0$$

and

$$x_2^{\ell} = -x_1^{\ell} \cot\theta + ((\ell-0.5)/k_1); \text{ for } 0<\theta\leq 90 \qquad (3.2\text{-}3)$$

where $\ell = 0, 1, 2, \ldots, (R_\theta+1)$, x_1 and x_2 are variables which denote the image coordinate system and ℓ denotes the ℓ-th line. In Fig. 3-2 we observe that the center of the ray #0 is always considered to pass through the point (0,0). For the purposes of illustration, the projection data for the case N=4 and projection angle $\theta=\tan^{-1}(1/2)$, i.e. $k_1=1$ and $k_2=2$ is shown in Fig. 2-4.

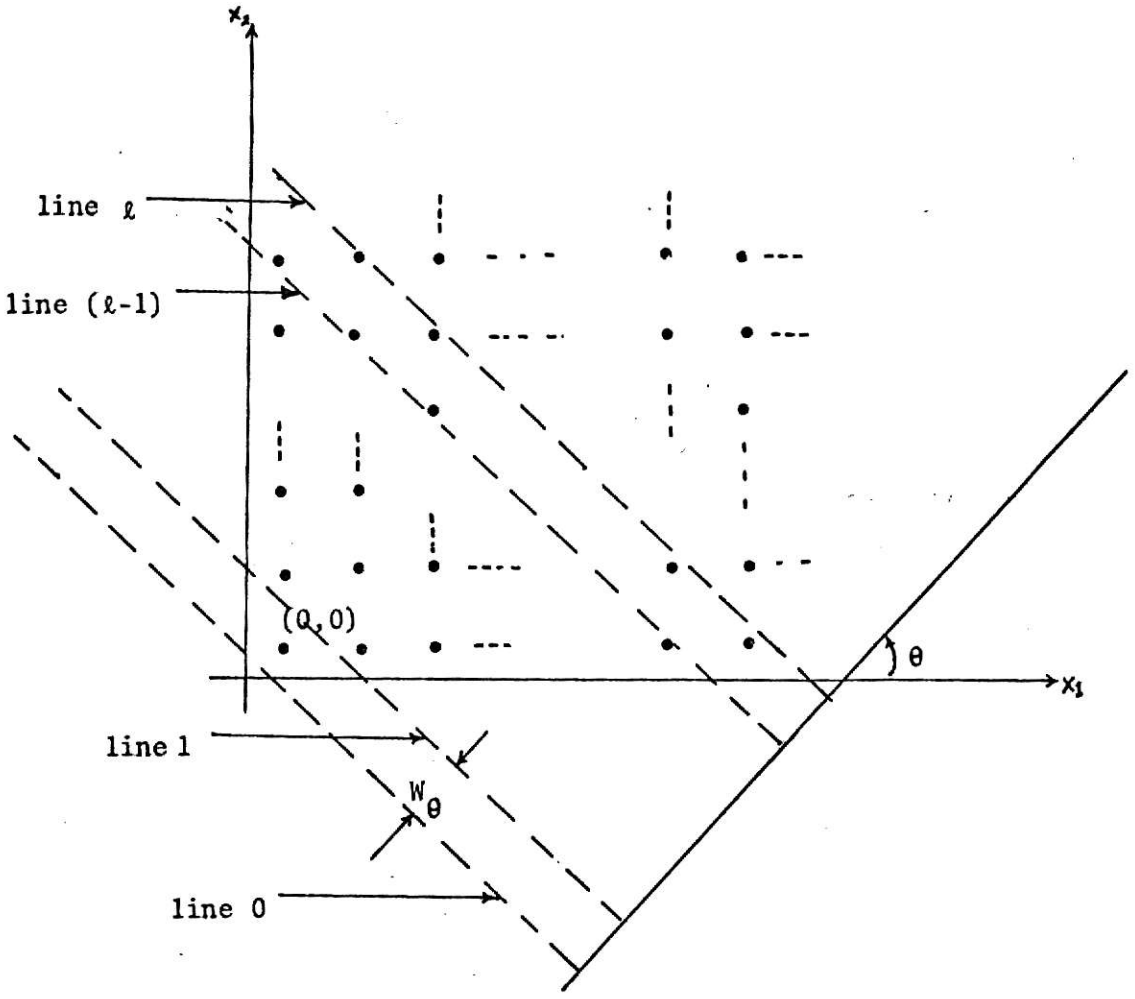

Fig. 3-2. Pertaining to line equations.

3.3. Simulation of Projection Data

The simulation of the projection data for a discrete NxN image at different projection angles can be performed by using the line equations in Eq. (3.2-3). Since the projection is the summation of densities contained within the ray, it is straightforward to compute the densities which are contained within a particular ray by computing the densities contained within two adjacent lines. The basic idea used for computing the desired densities is best explained by means of the following steps.

Step 1: Consider the initial density value $X(m_1,m_2)$ to be $X(0,0)$

Step 2: Consider the initial value of ℓ to be equal to -1.

Step 3: Increment the value of ℓ

Step 4: Compute the value of x_2^ℓ using Eq. (3.4-1) and $x_1^\ell=m_1$

Step 5: Compare the value of x_2^ℓ and m_1

Step 6: If the value of m_1 is more than x_2^ℓ then Go to step 3 otherwise go to step 7.

Step 7: As the value of m_1 is less than or equal to x_2^ℓ, assign the density value $X(m_1,m_2)$ to the $(\ell-1)$-th ray.

Step 8: Consider the density value of $X(m_1,m_2)$ in the same row and the next column.

Step 9: Consider the initial value of ℓ to be $(\ell-1)$ which had satisfied the condition in step 7.

Step 10: Go to step 3 until all the columns are computed for that row.

Step 11: Consider the density value of $X(m_1,m_2)$ from the next row and column #0.

Step 12: Increment the initial value of ℓ in step 2 and consider that as a new initial value in step 2; then repeat this process until all the rows of the image have been considered.

The above steps are conveniently summarized in Fig. 3-3. For example, let us consider the particular case N=4, k_1=1, k_2=2 and X(1,1). By using the line equations in Eq.(3.2-3) we obtain

$$x_2^0 = -2.5,\ x_2^1 = -1.5,\ x_2^2 = -0.5,\ x_2^3 = 0.5,\ x_2^4 = 1.5 \qquad (3.5\text{-}1)$$

As we compare the value of m_1 = 1 with different values of x_2^ℓ, which are given in Eq.(1), then it is observed that the value of m_1 is larger than x_2^ℓ up to ℓ=3. However, for ℓ =4, the value of m_1 = 1 is smaller than x_2^ℓ, so X(1,1) belongs to the 3-rd ray which is apparent from Fig. 2-4.

The above steps are implemented using Fortran as the programming language. The corresponding computer program subroutine PROJ is given in Appendix 3-1. The above technique is more general and can be used to implement the continuous case. However, there is another technique which is much faster in computation than the above technique, but it is restricted only for the discrete case. This technique uses an important property of the projection, which follows from section 2-4. It implies that the projection $P_\theta(s)$ at a particular angle θ is merely a summation of densities $X(m_1,m_2)$ for the values of m_1 and m_2 which satisfy the relation $k_1m_1+k_2m_2=s$, $s=0,1,\ldots,(N_\theta-1)$, where (k_1,k_2) is the critical grid point associated with projection angle θ. Hence the projection data is computed by using simple DO LOOPS. The corresponding computer program subroutine, PROJ1, implemented using Fortran as the programming language, is given in Appendix 3-2. Also, the Fortran program which implements the entire 3N/2-reconstruction algorithm is given in Appendix 3-3. This corresponding algorithm logic is summarized in Fig. 3-4.

For the purposes of illustration, we consider as the input data to the program in Appendix 3.3, for the 8x8 image given in Table 3-1. Then

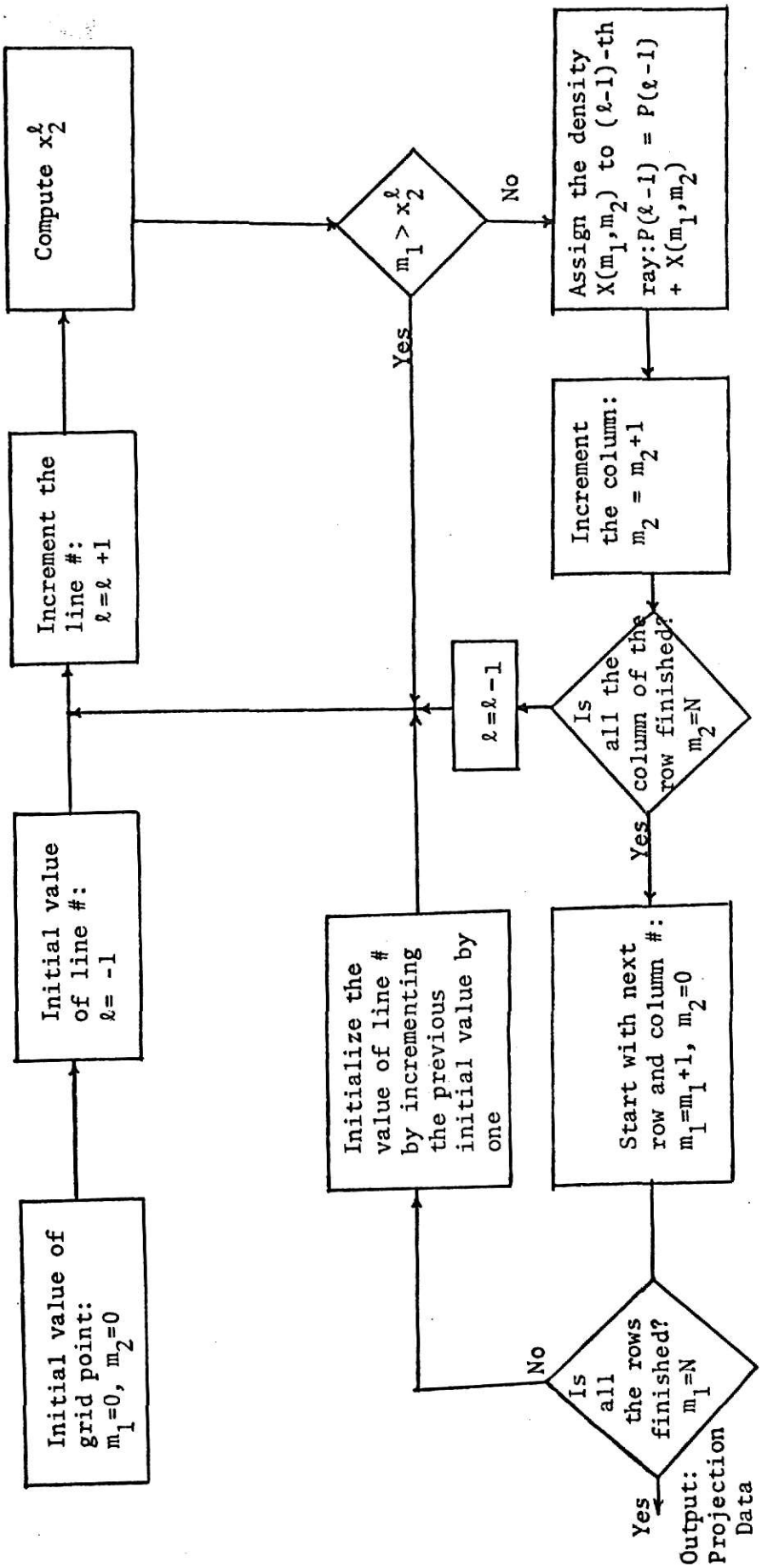

Fig. 3-3. Flowgraph for simulation of projection data.

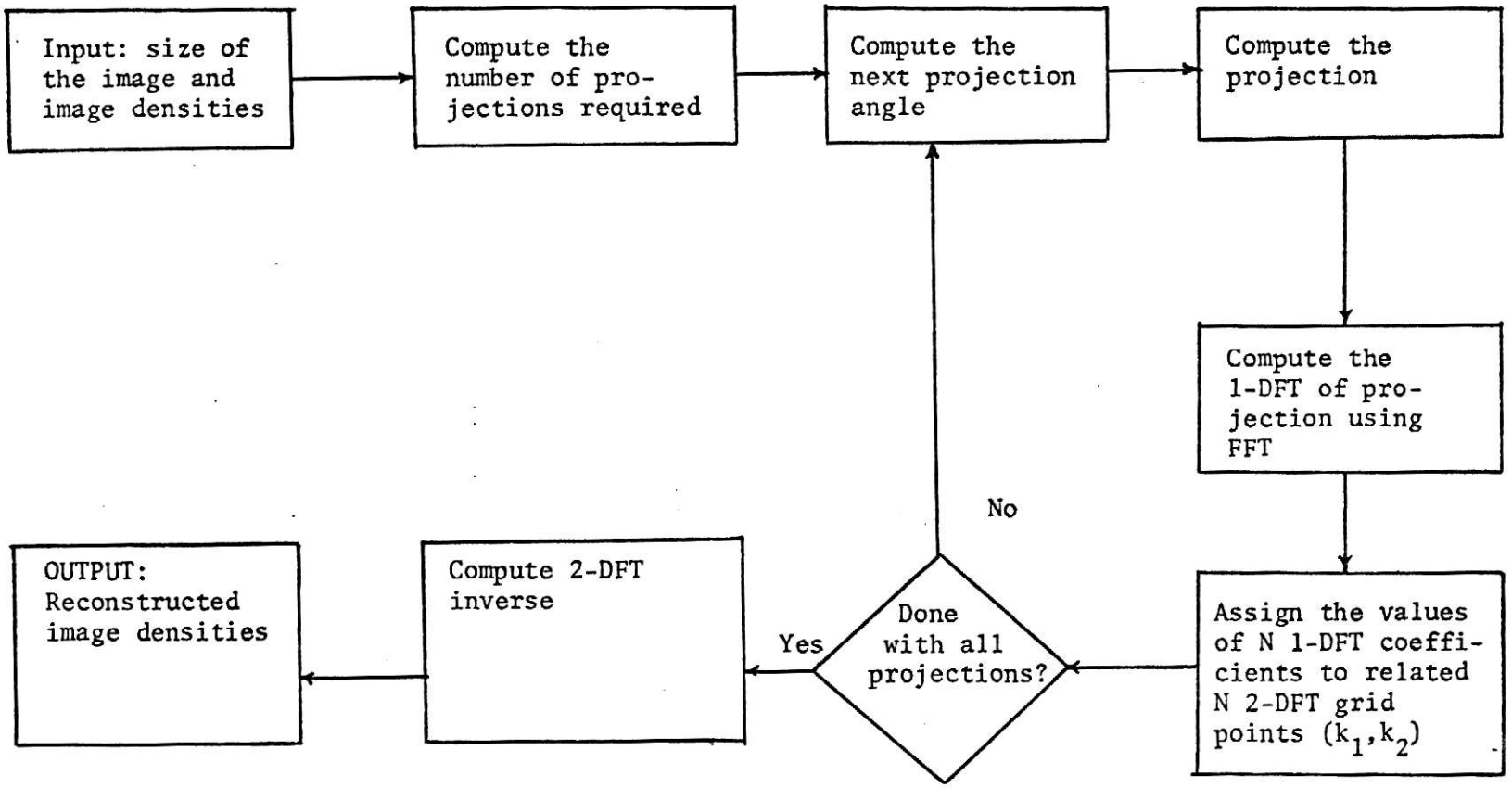

Fig. 3-4. Flowgraph for 3N/2- Reconstruction Algorithm.

the required angles, critical grid points, corresponding projections, and related 1-dimensional DFT coefficients are as summarized in Table 3.2.

Again, the 2-dimensional coefficients which are obtained from the above 1-dimensional projection are given in Table 3.3. Also, the inverse 2-dimensional DFT of this 2-dimensional coefficients are given in Table 3.4, from which it is apparent that reconstructed image is exactly the same as the original image given in Table 3.1.

TABLE 3.1

INPUT DENSITIES OF AN 8*8 IMAGE:

5.00	5.00	5.00	4.00	5.00	5.00	5.00	6.00
15.00	16.00	15.00	16.00	6.00	5.00	5.00	5.00
16.00	16.00	15.00	7.00	4.00	6.00	5.00	4.00
15.00	15.00	16.00	15.00	5.00	5.00	4.00	4.00
14.00	15.00	16.00	15.00	5.00	5.00	5.00	5.00
6.00	14.00	15.00	5.00	6.00	5.00	5.00	5.00
16.00	14.00	15.00	14.00	5.00	4.00	5.00	6.00
5.00	5.00	7.00	5.00	5.00	5.00	15.00	6.00

TABLE 3.2

1. PROJECTION ANGLE:90.00

CRITICAL GRID POINT (K1,K2): (1, 0)

PROJECTION:

40. 83. 73. 79. 80. 61. 79. 53.

1-DFT OF PROJECTION:

8.56+J0.0 -0.67-J0.44 -0.50-J0.19 -0.58-J0.62

-0.06+J0.0 -0.58+J0.62 -0.50+J0.19 -0.67+J0.44

2-DFT GRID PINTS:

(0, 0),(1, 0),(2, 0),(3, 0),(4, 0),(5, 0),(6, 0),(7, 0),

2. PROJECTION ANGLE:45.00

CRITICAL GRID POINT (K1,K2): (1, 1)

PROJECTION:

5. 20. 37. 50. 65. 55. 75. 71. 45. 40. 24. 19.

15. 21. 6.

1-DFT OF PROJECTION:

8.56+J0.0 -0.62+J0.51 -0.19+J0.06 -0.31-J0.11

-0.06+J0.0 -0.31+J0.11 -0.19-J0.06 -0.62-J0.51

2-DFT GRID PINTS:

(0, 0),(1, 1),(2, 2),(3, 3),(4, 4),(5, 5),(6, 6),(7, 7),

TABLE 3.2 (CCNT.)

```
 3. PROJECTION ANGLE:26.57
CRITICAL GRID PCINT (K1,K2): ( 1, 2)
PROJECTICN:
  5.  15.  21.  31.  35.  36.  50.  51.  42.  41.  39.  22.
 30.  21.  21.  19.  13.  14.  10.  20.   6.   6.
1-DFT OF PROJECTION:
  8.56+J0.0        -0.13-J0.09       -0.16+J0.16       -0.22-J0.13
 -0.C6+J0.0        -C.22+J0.13       -0.16-J0.16       -0.13+J0.09
2-DFT GRID PINTS:
 ( C, 0),( 1, 2),( 2, 4),( 3, 6),( 4, 0),( 5, 2),( 6, 4),( 7, 6),

 4. PRCJECTICN ANGLE:18.43
CRITICAL GRID PCINT (K1,K2): ( 1, 3)
PROJECTION:
  5.  15.  16.  20.  30.  22.  36.  35.  29.  34.  37.  22.
 35.  28.   9.  24.  15.  12.  15.  15.  10.  14.  15.   9.
  9.  20.   5.   6.   6.
1-DFT OF PROJECTION:
  8.56+J0.0        -0.12-J0.34       0.09-J0.22        -0.60+J0.07
 -0.C6+J0.0        -C.60-J0.07       0.09+J0.22        -0.12+J0.34
2-DFT GRID PINTS:
 ( 0, 0),( 1, 3),( 2, 6),( 3, 1),( 4, 4),( 5, 7),( 6, 2),( 7, 5),
```

TABLE 3.2 (CONT.)

```
 5. PROJECTION ANGLE:14.04
CRITICAL GRID POINT (K1,K2): ( 1, 4)
PROJECTION:
  5.  15.  16.  15.  19.  22.  32.  20.  20.  29.  29.  21.
 20.  31.  22.  22.  20.  11.  18.  10.  10.  11.  11.  10.
 10.  10.   9.   9.  11.  10.   9.  19.   5.   5.   6.   6.
1-DFT OF PROJECTION:
  8.56+J0.0          0.07+J0.09        -0.50-J0.19        -0.07+J0.22
 -0.06+J0.0         -0.07-J0.22        -0.50+J0.19         0.07-J0.09
2-DFT GRID PINTS:
 ( 0, 0),( 1, 4),( 2, 0),( 3, 4),( 4, 0),( 5, 4),( 6, 0),( 7, 4),

 6. PROJECTION ANGLE:11.31
CRITICAL GRID POINT (K1,K2): ( 1, 5)
PROJECTION:
  5.  15.  16.  15.  14.  11.  32.  21.  15.  15.  19.  29.
 20.  16.  16.  19.  31.  14.  15.  15.  10.  20.   9.   5.
  5.  11.  10.  11.   5.   5.  10.   9.  10.   4.   5.  11.
 10.  19.   4.   5.   5.   6.   6.
1-DFT OF PROJECTION:
  8.56+J0.0         -0.12-J0.18        -0.19+J0.06         0.50-J0.18
 -0.06+J0.0          0.50+J0.18        -0.19-J0.06        -0.12+J0.18
2-DFT GRID PINTS:
 ( 0, 0),( 1, 5),( 2, 2),( 3, 7),( 4, 4),( 5, 1),( 6, 6),( 7, 3),
```

TABLE 3.2 (CONT.)

```
 7. PROJECTION ANGLE: 9.46
CRITICAL GRID POINT (K1,K2): ( 1, 6)
PROJECTION:
  5.  15.  16.  15.  14.   6.  21.  21.  16.  15.  15.  14.
 19.  20.  15.  16.  16.  15.  19.  23.   7.  15.  15.   5.
 19.  11.   4.   5.   5.   6.  10.  10.   6.   5.   5.   5.
  9.  10.   5.   4.   5.   5.  11.  20.   4.   4.   5.   5.
  6.   6.
1-DFT OF PROJECTION:
  8.56+J0.0          0.12-J0.34         -0.16+J0.16          0.34-J0.37
 -0.06+J0.0          0.34+J0.37         -0.16-J0.16          0.12+J0.34
2-DFT GRID PINTS:
 ( 0, 0),( 1, 6),( 2, 4),( 3, 2),( 4, 0),( 5, 6),( 6, 4),( 7, 2),

 8. PROJECTION ANGLE: 8.13
CRITICAL GRID POINT (K1,K2): ( 1, 7)
PROJECTION:
  5.  15.  16.  15.  14.   6.  16.  10.  16.  16.  15.  15.
 14.  14.  10.  15.  15.  16.  16.  15.  15.  11.  16.   7.
 15.  15.   5.  14.  10.   6.   4.   5.   5.   6.   5.  10.
  5.   6.   5.   5.   5.   4.  10.   5.   5.   4.   5.   5.
  5.  21.   5.   4.   4.   5.   5.   6.   6.
1-DFT OF PROJECTION:
  8.56+J0.0          0.25-J0.90          0.09-J0.22         -0.10-J0.56
 -0.06+J0.0         -0.10+J0.56          0.09+J0.22          0.25+J0.90
2-DFT GRID PINTS:
 ( 0, 0),( 1, 7),( 2, 6),( 3, 5),( 4, 4),( 5, 3),( 6, 2),( 7, 1),
```

TABLE 3.2 (CONT.)

```
 9. PROJECTION ANGLE: 0.0
CRITICAL GRID POINT (K1,K2): ( 0, 1)
PROJECTION:
 92. 100. 104.  81.  41.  40.  49.  41.
1-DFT OF PROJECTION:
  8.56+J0.0        1.02-J1.96       -0.31-J0.28        0.58-J0.25
  0.38+J0.0        0.58+J0.25       -0.31+J0.28        1.02+J1.96
2-DFT GRID PINTS:
 ( 0, 0),( 0, 1),( 0, 2),( 0, 3),( 0, 4),( 0, 5),( 0, 6),( 0, 7),

10. PROJECTION ANGLE:63.43
CRITICAL GRID POINT (K1,K2): ( 2, 1)
PROJECTION:
  5.   5.  20.  20.  36.  37.  41.  33.  39.  41.  32.  38.
 40.  28.  31.  29.  17.  14.  10.  11.  15.   6.
1-DFT OF PROJECTION:
  8.56+J0.0       -0.67+J0.20        0.28+J0.0        -0.27-J0.11
  0.38+J0.0       -0.27+J0.11        0.28+J0.0        -0.67-J0.20
2-DFT GRID PINTS:
 ( 0, 0),( 2, 1),( 4, 2),( 6, 3),( 0, 4),( 2, 5),( 4, 6),( 6, 7),
```

TABLE 3.2 (CCNT.)

11. PROJECTION ANGLE:75.96

CRITICAL GRID PCINT (K1,K2): (4, 1)

PROJECTION:

5. 5. 5. 4. 20. 21. 20. 22. 22. 21. 20. 12.

19. 21. 21. 19. 19. 20. 20. 19. 11. 19. 20. 10.

22. 19. 20. 19. 10. 9. 12. 11. 5. 5. 15. 6.

1-DFT CF PRCJECTICN:

8.56+J0.0 0.23-J0.09 -0.31-J0.28 0.18+J0.13

0.38+J0.0 0.18-J0.13 -0.31+J0.28 0.23+J0.09

2-DFT GRID PINTS:

(0, 0),(4, 1),(0, 2),(4, 3),(C, 4),(4, 5),(0, 6),(4, 7),

12. PROJECTICN ANGLE:80.54

CRITICAL GRID POINT (K1,K2): (6, 1)

PROJECTICN:

5. 5. 5. 4. 5. 5. 20. 22. 15. 16. 6. 5.

21. 21. 15. 7. 4. 6. 20. 19. 16. 15. 5. 5.

18. 19. 16. 15. 5. 5. 11. 19. 15. 5. 6. 5.

21. 19. 15. 14. 5. 4. 10. 11. 7. 5. 5. 5.

15. 6.

1-DFT OF PRCJECTICN:

8.56+J0.0 0.C8+J0.37 0.28+J0.C -0.01+J0.12

0.38+J0.0 -0.01-J0.12 0.28+J0.0 0.C8-J0.37

2-DFT GRID PINTS:

(0, 0),(6, 1),(4, 2),(2, 3),(0, 4),(6, 5),(4, 6),(2, 7),

TABLE 3.3

2-DFT COEFFICIENTS OBTAINED VIA 1-DFTOF PROJECTIONS:

8.56+J0.0	-0.67-J0.44	-0.50-J0.19	-0.58-J0.62
-0.06+J0.0	-0.58+J0.62	-0.50+J0.19	-0.67+J0.44
1.02-J1.96	-0.62+J0.51	-0.67+J0.20	-0.60+J0.07
0.23-J0.09	0.50+J0.18	0.08+J0.37	0.25+J0.90
-0.31-J0.28	-0.13-J0.09	-0.19+J0.06	0.34-J0.37
0.28+J0.0	-0.22+J0.13	0.09+J0.22	0.12+J0.34
0.58-J0.25	-0.12-J0.34	-0.01+J0.12	-0.31-J0.11
0.18+J0.13	-0.10+J0.56	-0.27-J0.11	-0.12+J0.18
0.38+J0.0	0.07+J0.09	-0.16+J0.16	-0.07+J0.22
-0.06+J0.0	-0.07-J0.22	-0.16-J0.16	0.07-J0.09
0.58+J0.25	-0.12-J0.18	-0.27+J0.11	-0.10-J0.56
0.18-J0.13	-0.31+J0.11	-0.01-J0.12	-0.12+J0.34
-0.31+J0.28	0.12-J0.34	0.09-J0.22	-0.22-J0.13
0.28+J0.0	0.34+J0.37	-0.19-J0.06	-0.13+J0.09
1.02+J1.96	0.25-J0.90	0.08-J0.37	0.50-J0.18
0.23+J0.09	-0.60-J0.07	-0.67-J0.20	-0.62-J0.51

TABLE 3.4

RECONSTRECTED DENSITIES FOR AN 8*8 IMAGE:

5.00	5.00	5.00	4.00	5.00	5.00	5.00	6.00
15.00	16.00	15.00	16.00	6.00	5.00	5.00	5.00
16.00	16.00	15.00	7.00	4.00	6.00	5.00	4.00
15.00	15.00	16.00	15.00	5.00	5.00	4.00	4.00
14.00	15.00	16.00	15.00	5.00	5.00	5.00	5.00
6.00	14.00	15.00	5.00	6.00	5.00	5.00	5.00
16.00	14.00	15.00	14.00	5.00	4.00	5.00	6.00
5.00	5.00	7.00	5.00	5.00	5.00	15.00	6.00

CHAPTER IV

CONCLUSIONS AND RECOMMENDATIONS

4.1. Conclusions

The main results presented in this research study pertain to the reconstruction of noiseless, bandlimited digital images from their projections, using a Fourier approach. It has been shown that an (NxN) image can be reconstructed from either a set of 3N/2 projections, or a single projection, without resorting to any tedious computational techniques. The result pertaining to the 3N/2 projections is in agreement with a conjecture by Mersereau which states that exact reconstruction should be possible when the number of projections is in the order of N/2 [3]. Again, the single projection result is consistent with the one projection theorem developed by Mersereau [3]. However, in this case it is shown that a particular projection yields projection data which corresponds to the rows of the given image arranged in lexicographical order. As a consequence, the resulting reconstruction algorithm requires no tedious calculations, as is the case with the one projection theorem approach [3]. It is equivalent to the conventional algorithm for computing the 2-dimensional DFT using 2N applications of a 1-dimensional FFT of size N, where the corresponding algorithm is derived via a matrix Kronecker product formulation.

It is important to note that the 3N/2 projection reconstruction formulation presented in this study differs from previous formulations in two respects:

(i) The projection angle $\theta=\tan^{-1}(k_1/k_2)$ is a function of frequency numbers k_1 and k_2. In previous attempts θ was independent of

k_1 and k_2.

(ii) The ray width is also the function of frequency numbers k_1 and k_2 [see Eq.(3.2-1)]; again, in previous studies ray width was independent of k_1 and k_2, though it was dependent on θ in some cases.

Examination of Eq.(2.5-4) reveals that the subset of projection angles given by

$$\theta = \tan^{-1}(k_1/k_2) \qquad (4.1\text{-}1)$$

where $k_1 = 1$ and $k_2 = m$, $m=0,1,\ldots,(N-1)$ becomes smaller with increasing N. Clearly, this could lead to the situation where the difference between successive projection angles is too small and unrealizable in practice. In such cases a search for a more suitable critical set is suggested, as illustrated for the (8x8) case in Fig. 4-1. Figure 4-1(a) shows the critical set which is obtained directly from Eq.(2.5-4), along with the corresponding differences between successive θ. However, if we consider the alternate critical set

$$\left\{\begin{matrix}(0,1),\ (1,1),\ (1,2),\ (1,3),\ (3,4),\ (1,5), \\ (3,2),\ (1,7),\ (1,0),\ (1,2),\ (4,1),\ (6,1)\end{matrix}\right\} \qquad (4.1\text{-}2)$$

we observe that the corresponding differences between successive θ are somewhat higher, as summarized in Fig. 4-1(b). We remark that the above alternate critical set is obtained by replacing the critical grid points (1,4) and (1,6) in Fig. 4-1(a) by congruence

$$(3,4) = (3\text{x}1(\text{mod } 8),\ 3\text{x}4(\text{mod } 8))$$

and $(3,2) = (3\text{x}1(\text{mod } 8),\ 3\text{x}6(\text{mod } 8))$ respectively.

#	Critical gridpoints (k_1,k_2)	Projection angles $\theta = \tan^{-1}(k_1/k_2)$	Differences
1.	(0,1)	0.0	
2.	(1,7)	8.13	8.13
3.	(1,6)	9.46	1.33
4.	(1,5)	11.31	1.85
5.	(1,4)	14.04	2.73
6.	(1,3)	18.43	4.39
7.	(1,2)	26.56	8.13
8.	(1,1)	45.00	18.44
9.	(2,1)	63.43	18.43
10.	(4,1)	75.96	12.53
11.	(6,1)	80.53	4.57
12.	(1,0)	90.00	9.47

(a)

1.	(0,1)	0.0	
2.	(1,7)	8.13	8.13
3.	(1,5)	11.31	3.18
4.	(1,3)	18.43	7.12
5.	(1,2)	26.56	8.13
6.	(3,4)	36.87	10.31
7.	(1,1)	45.00	8.13
8.	(3,2)	56.31	11.31
9.	(2,1)	63.43	7.12
10.	(4,1)	25.96	12.53
11.	(6,1)	80.53	4.57
12.	(1,0)	90.00	9.47

(b)

Fig. 4-1. Critical grid points, associated projection angles, and differences between two successive projection angles for N = 8.

4.2. Recommendations for Further Investigation

There are at least three problems that deserve to be investigated in connection with the 3N/2-Reconstruction Algorithm. These problems can be summarized as follows:

(i) The present analysis has been restricted to noiseless digital images. An attempt to extend the analysis to the noisy case would be beneficial. A basic problem one encounters in such an extension is that related to the estimation of certain 2-dimensional DFT coefficients which result from more than one projection. In the noiseless case, such coefficients pose no problem since their values are the same regardless of the projection angle. However, when noise is present, their values will depend on θ, and will hence have to be evaluated via an appropriate estimation technique.

(ii) In the above formulation, parallel rays are assumed. However, in cases where the distance between the radiation source and the object is not sufficiently large, a fan beam is obtained rather than a parallel beam. In such cases it would be necessary to suitably modify the 3N/2-Reconstruction Algorithm so as to be able to handle the fan beam situation.

(iii) In the area of transform coding of images, the 2-dimensional DFT of an (NxN) image block is typically computed via 2N successive applications of a 1-dimensional FFT. This results in a set of N^2 transform components of which a function is selected for coding purposes, and the remaining are discarded. It is plausible that a small set of projections can be used to directly compute the desired subset of N^2 transform components, as opposed to first computing the entire set of N^2 transform components and then selecting the desired subset.

REFERENCES

[1] N. Ahmed and K. R. Rao, "Orthogonal Transforms for Digital Signal Processing," 1975.

[2] T. F. Budinger, et al., "Three-Dimensional Reconstruction in Nuclear Medicine by Iterative Least-Squares and Fourier Transform Techniques," Lawrence Berkeley Laboratory, Rept. #TID-4500-R61, Jan. 1974.

[3] R. M. Mersereau and A. V. Openheim, "Digital Reconstruction of Multidimensional Signals from their Projections," Proc. IEEE, Oct. 1974, pp. 1319-1338.

[4] R. M. Mersereau, "Recovering Multidimensional Signals from their Projections," Computer Graphics and Image Processing, 1973, pp. 179-195.

[5] R. M. Mersereau and D. E. Dudgeon, "The Representation of Two-Dimensional Sequences as One-Dimensional Sequences," IEEE Trans. Acoustics, Speech and Signal Processing, Vol. ASSP-22, Oct. 1974, pp. 320-325.

[6] R. Gordon, R. Bender, and G. T. Herman, "Algebraic reconstruction techniques (ART) for three-dimensional electron microscopy and X-ray photography," J. Theor. Biol., vol. 29, pp. 471-481, 1970.

[7] P. Gilbert, "Iterative methods for the three-dimensional reconstruction of an object from projections," J. Theor. Biol., vol. 36, pp. 105-117.

[8] G. T. Herman, "Two direct methods for reconstructing pictures from their projections: A comparative study," Comp. Graph. Image Proc., vol. 1, pp. 123-144, 1973.

[9] G. N. Ramachandran and A. V. Lakshminarayanan, "Three-dimensional reconstruction from radiographs and electron micrographs: II. Application of convolutions instead of Fourier transforms," Proc. Nat. Acad. Sci., vol. 68, no. 9, pp. 2236-2240.

[10] S. W. Rowland, "SNARK - A Picture Reconstruction Framework," Dept. Rept. #51-72, Sept. 1972, Dept. of Computer Science, State University of New York at Buffalo, Amherst, New York 14226.

[11] B. K. Vainshtein, "Finding the structure of objects from projections," Sov. Phys.-Crystall., vol. 15, no. 5, pp. 781-787.

[12] R. N. Bracewell, "Strip integration in radio astronomy," Aust. J. Phys., vol. 9, pp. 198-217, 1956.

[13] D. J. DeRosier and A. Klug, "Reconstruction of three-dimensional structures from electron micrographs," Nature, vol. 217, pp. 130-134, 1968.

[14] R. A. Crowther, D. J. DeRosier, and A. Klug, "The reconstruction of a three-dimensional structure from projections and its application to electron microscopy," Proc. Roy. Soc. London, Ser. A, vol. 317, pp. 319-340, 1970.

[15] T. F. Budinger, "Transfer function theory in image evaluation in Biology-Applications in electron microscopy and nuclear medicine," Ph.D. thesis, University of California, Berkeley, 1971.

[16] J. A. Lake, "Reconstruction of three-dimensional structures from sectioned helices by deconvolution of partial data," J. Mol. Biol., vol. 66, pp. 255-269, 1972.

[17] T. M. Peters, "Image reconstruction from projections," Ph.D. thesis, University of Canterbury, Christ Church, New Zealand, 1973.

[18] T. Natarajan, "Interframe transform coding of monochrome pictures," Ph.D. dissertation, E. E. Dept., Kansas State University, Manhattan, Kansas, 1976.

ILLEGIBLE

THE FOLLOWING DOCUMENT(S) ARE ILLEGIBLE DUE TO THE PRINTING ON THE ORIGINAL BEING CUT OFF

THIS IS AS RECEIVED FROM THE CUSTOMER AND IS THE BEST POSSIBLE IMAGE AVAILABLE

ILLEGIBLE

APPENDIX 3.1

```
      SUBROUTINE PRCJ(X,PR,NL,N)
C
C     THIS SUBROUTINE CALCULATES THE PROJECTION FOR THE GIVEN
C     CRITICAL GRID POINT (K1,K2)
C
      DIMENSION X(64,64),PR(1)
      COMMON K1,K2
C
C     CALCULATE # OF RADIATION LINES
C
      NL=(K1+K2)*(N-1)+2
      DO 11 I=1,NL
   11 PR(I)=0.
      NO=0
      IF(K1.EQ.0) GO TO 100
C
C     CALCULATES THE PROJECTION FOR 0<THETA=<90.
C
      DO 12 M1=1,N
      NS=NC+1
      X2=FLOAT(M1-1)
      DO 13 M2=1,N
      X1=FLOAT(M2-1)
      DO 14 L=NS,NL
      X2C=(FLOAT(L-1)-.5-(FLOAT(K2)*X1))/FLOAT(K1)
      IF(X2C.LT.X2) GO TO 14
      PR(L-1)=PR(L-1)+X(M1,M2)
      GO TO 113
   14 CONTINUE
  113 NS=L
   13 CONTINUE
      NO=NO+1
   12 CONTINUE
      RETURN
C
C     CALCULATES THE PROJECTION FOR THETA=0
C
  100 DO 17 M2=1,N
      NS=NC+1
      X1=FLOAT(M2-1)
      DO 18 M1=1,N
      DO 19 L=NS,NL
      X1C=FLOAT(L-1)-.5
      IF(X1C.LT.X1)GO TO 19
      PR(L-1)=PR(L-1)+X(M1,M2)
      GO TO 118
   19 CONTINUE
  118 NS=L
   18 CONTINUE
      NO=NC+1
   17 CONTINUE
      RETURN
      END
```

APPENDIX 3.2

```
      SUBRCUTINE PRCJ1(X,PR,N,NL)
C
C     THIS SUBROUTINE CCMPUTES THE PROJECTION DATA OF AN (NXN)
C     DIGITAL IMAGE FOR A GIVEN VALUE CF CRITICAL GRID POINT (K1,K2)
C
      DIMENSION X(64,64),PR(1)
      COMMCN K1,K2
      NL=(K1+K2)*(N-1)+1
      DO 10 I=1,NL
   10 PR(I)=0.0
      DO 11 M1=1,N
      DO 12 M2=1,N
      KK=K1*(M1-1)+K2*(M2-1)
      KK=KK+1
   12 PR(KK)=PR(KK)+X(M1,M2)
   11 CONTINUE
      RETURN
      END
```

APPENDIX 3.3

```
C
C     THIS PROGRAM IMPLEMENTS THE 3N/2 - RECONSTRUCTION ALGORITHM
C
      DIMENSION D(64,64),AIM(64)
      DIMENSION RE(64),PR(4096)
      INTEGER*2 IND1(64),IND2(64)
      COMPLEX X(4096),Y(4096),CX(64,64),CMPLX
      EQUIVALENCE (Y(1),CX(1,1))
      COMMON K1,K2
      INTEGER*2 JPS/'+J'/,JNS/'-J'/
      INTEGER*2 JS(64)
      READ 11,N,((D(I,J),J=1,N),I=1,N)
   11 FORMAT(I3/(16F2.0))
      PRINT 1
    1 FORMAT('1',///,(' ',36X,'TABLE 3.1'))
      PRINT 2,((D(I,J),J=1,N),I=1,N)
    2 FORMAT('0',13X,'INPUT DENSITIES OF AN 8*8 IMAGE:',//,
     X('0',10X,8F8.2))
      NN=N*N
      NP=3*N/2
      MCON=0
      DO 100 IP=1,NP
C
C     CALCULATE THE PROJECTION ANGLE AND CRITICAL GRID POINT
C
      CALL CRGRID(IP,ANG,N)
C
C     CALCULATE THE PROJECTION
C
      CALL PROJ(D,PR,NL,N)
C
C     CALCULATE THE SMALLEST INTEGER # OF THE ORDER OF 2**N ,
C     EQUAL TO OR GREATER THAN NL
C
      CALL POWER2(N,NL,PR,NT,X)
C
C     CALCULATE THE 1-DFT OF PROJECTION VECTOR USING FFT ALGORITHM
C
      CALL FFT(X,NT,0,NN)
C
C     CALCULATE THE N 2-DFT COEFFICIENT
C
      CALL TWODFT(N,NT,X,CX,IND1,IND2)
      MCON=1-MCON
      IF(MCON.EQ.1) PRINT 13
   13 FORMAT('1',//,(' ',36X,'TABLE 3.2 (CONT.)'))
      PRINT 14,IP,ANG
   14 FORMAT ('-',13X,I2,'. ','PROJECTION ANGLE:',F5.2)
      PRINT 15,K1,K2
   15 FORMAT('0',13X,'CRITICAL GRID POINT (K1,K2): (',I2,',',I2,')')
      PRINT 16,(PR(I),I=1,NL)
   16 FORMAT('0',13X,'PROJECTION:'/('0',12X,12F5.0))
```

```
      NJ=NT/N
      DO 31 I=1,N
   31 JS(I)=JNS
      KK=0
      DO 33 I=1,NT,NJ
      KK=KK+1
      RE(KK)=REAL(X(I))
      AIM(KK)=AIMAG(X(I))
      IF(AIM(KK).GE.0.)JS(KK)=JPS
   33 AIM(KK)=ABS(AIM(KK))
      PRINT 35,(RE(I),JS(I),AIM(I),I=1,N)
   35 FORMAT('0',13X,'1-DFT OF PROJECTION:'/
     X('0',14X,4(F5.2,A2,F4.2,6X)))
      PRINT 23,(IND1(I),IND2(I),I=1,N)
   23 FORMAT('0',13X,'2-DFT GRID PINTS:',/,('0',14X,8('(',I2,',',I2
     X,')',',')))
  100 CONTINUE
      PRINT 18
   18 FORMAT('1',///,(' ',36X,'TABLE 3.3'))
      PRINT 41
   41 FORMAT('-',13X,'2-DFT COEFFICIENTS OBTAINED VIA 1-DFT',
     X'OF PROJECTIONS:')
      J2=0
      DO 43 I=1,N
      J1=J2+1
      J2=J2+N
      DO 44 J=1,N
   44 JS(J)=JNS
      KK=0
      DO 45 J=J1,J2
      KK=KK+1
      RE(KK)=REAL(Y(J))
      AIM(KK)=AIMAG(Y(J))
      IF(AIM(KK).GE.0.)JS(KK)=JPS
   45 AIM(KK)=ABS(AIM(KK))
      PRINT 46,(RE(J),JS(J),AIM(J),J=1,N)
   46 FORMAT('-',14X,4(F5.2,A2,F4.2,5X),/,
     X15X,4(F5.2,A2,F4.2,5X))
   43 CONTINUE
C
C     CALCULATE THE 2-DIMENSIONAL INVERS DFT USING IFFT
C
      CALL I2DFT(Y,N)
      PRINT 40
   40 FORMAT('1',///,(' ',36X,'TABLE 3.4'))
      PRINT 19
   19 FORMAT('-',13X,'RECONSTRECTED DENSITIES FOR AN 8*8 IMAGE:')
      DO 20 I=1,N
      J1=(I-1)*N+1
      J2=I*N
      KK=0
      DO 24 J=J1,J2
      KK=KK+1
   24 RE(KK)=REAL(Y(J))
      PRINT 21,(RE(J),J=1,N)
   21 FORMAT ('0',10X,8F8.2)
   20 CONTINUE
      STOP
      END
```

```
      SUBROUTINE CRGRID(IP,ANG,N)
      COMMON K1,K2
C
C     THIS SUBROUTINE CALCULATES THE CRITICAL GRID POINT AND
C     RELATED ANGLE THETA
C
      PI=4.*ATAN(1.)
      IF(IP.GT.N) GO TO 1
      K1=1
      K2=IP-1
      IF(K2.EQ.0) GO TO 3
      GO TO 2
    1 K2=1
      K1=(IP-N-1)*2
    2 ANG=ATAN(FLOAT(K1)/FLOAT(K2))
      ANG=ANG*180./PI
      RETURN
    3 ANG=90.
      RETURN
      END



      SUBROUTINE FFT(X,N,INV,M1)
C
C     THIS PROGRAM IMPLEMENTS THE FFT ALGORITHM TO COMPUTE THE
C     DISCRETE FOURIER COEFFICIENTS OF DATA SEQUENCE OF N POINTS
C
      COMPLEX X(1),W,T,CMPLX
C
C     CALCULATE THE # OF ITERATIONS (LOG.  N  TO THE BASE 2.)
C
      ITER=0
      IREM=N
   10 IREM=IREM/2
      IF (IREM.EQ.0) GO TO 20
      ITER=ITER+1
      GO TO 10
   20 CONTINUE
      SIGN=-1.
      IF (INV.EQ.1) SIGN=1.
      NXP2=N
      DO 50 IT=1,ITER
C
C     COMPUTATION FOR EACH ITERATION
C     NXP: NUMBER OF POINTS IN A PARTITION
C     NXP2: NXP/2
C
      NXP=NXP2
      NXP2=NXP/2
      WPWR=3.141592/FLOAT(NXP2)
      DO 40 M=1,NXP2
C
C     CALCULATE THE MULTIPLIER
C
      ARG=FLOAT(M-1)*WPWR
      W=CMPLX(COS(ARG),SIGN*SIN(ARG))
      DO 40 MXP=NXP,N,NXP
C
```

```
C      COMPUTATION   FOR EACH PARTITION
C
       J1=MXP-NXP+M
       J2=J1+NXP2
       T=X(J1)-X(J2)
       X(J1)=X(J1)+X(J2)
   40  X(J2)=T*W
   50  CONTINUE
C
C      UNSCRAMBLE THE BIT-REVERSED DFT COEFFS.
C
       N2=N/2
       N1=N-1
       J=1
       DO 65 I=1,N1
       IF(I.GE.J) GO TO 55
       T=X(J)
       X(J)=X(I)
       X(I)=T
   55  K=N2
   60  IF(K.GE.J) GO TO 65
       J=J-K
       K=K/2
       GO TO 60
   65  J=J+K
       IF (INV.EQ.1) GO TO 75
       DO 70 I=1,N
   70  X(I)=X(I)/FLOAT(M1)
   75  CONTINUE
       RETURN
       END


       SUBROUTINE POWER2(N,NL,PR,NT,X)
C
C      THIS SUBROUTINE CALCULATES THE SMALLEST INTEGER
C      OF POWER 2,WHICH IS GREATER THAN OR EQUAL TO # OF
C      ELEMENTS IN PROJECTION VECTOR
C
       DIMENSION PR(1)
       COMPLEX X(1),CMPLX
       NL=NL-1
       DO 12 I=1,NL
   12  X(I)=CMPLX(PR(I),0.0)
       NT=N
    2  IF(NL.LE.NT) GO TO 3
       NT=NT*2
       GO TO 2
    3  IF(NL.EQ.NT) GO TO 5
       NN=NL+1
       DO 13 I=NN,NT
   13  X(I)=0.
    5  RETURN
       END


       SUBROUTINE TWODFT(N,NT,X,CX,IND1,IND2)
C
```

```
C     THIS SUBROUTINE CALCULATES THE N 2-DIMENSIONAL GRID POINTS
C     ASSOCIATED WITH CRITICAL GRID POINT (K1,K2)
C
      INTEGER*2 IND1(1),IND2(1)
      COMPLEX CX(N,N),X(1),CMPLX
      COMMON K1,K2
      DO 14 I=1,N
      INDX1=K1*(I-1)
      INDX2=K2*(I-1)
    2 IF(INDX1.LT.N) GO TO 1
      INDX1=INDX1-N
      GO TO 2
    1 IF(INDX2.LT.N)GO TO 3
      INDX2=INDX2-N
      GO TO 1
    3 CX(INDX1+1,INDX2+1)=X(((I-1)*NT/N)+1)
      IND1(I)=INDX1
      IND2(I)=INDX2
   14 CONTINUE
      RETURN
      END



      SUBROUTINE I2DFT(X,N)
C
C     THIS SUBROUTINE COMPUTES THE INVERS 2-DFT OF THE
C     2- DIMENSIONAL DISCRETE FOURIER COEFFICIENTS
C     OF AN (NXN) ARRAY
C
      COMPLEX X(1),MULT(32)
      NH=N/2
      CALL WPOWER(MULT,NH,1)
      LOG2N=LOG2(N)
      DO 100 ID=1,2
      CALL ONEDT(X,N,LOG2N,MULT)
      CALL SHFLNN(X,N)
  100 CONTINUE
      RETURN
      END



      SUBROUTINE ONEDT(X,N,LOG2N,MULT)
      COMPLEX X(1),MULT(1)
      IND=-N+1
      DO 50 IN=1,N
      INC=IND+N
      CALL IFFT(X(INC),N,LOG2N,MULT)
   50 CONTINUE
      RETURN
      END



      SUBROUTINE SHFLNN(X,N)
      COMPLEX X(1),T
      N1=N-1
      DO 50 IN=1,N1
      IN1=IN+1
```

```
      I2=IN*N
      I1=I2-N+IN1
      J=I1+N1
      DO 20 I=I1,I2
      T=X(I)
      X(I)=X(J)
      X(J)=T
   20 J=J+N
   50 CONTINUE
      RETURN
      END
      FUNCTION LOG2(N)
      LOG2=0
      N2=N
   10 N2=N2/2
      IF(N2.EQ.0) GO TO 15
      LOG2=LOG2+1
      GO TO 10
   15 RETURN
      END


      SUBROUTINE IFFT(X,N,NITER,MULT)
      COMPLEX X(1),MULT(1),W,T
      NXP2=N
      INC=1
      DO 50 IT=1,NITER
      NXP=NXP2
      NXP2=NXP2/2
      IP=1
      DO 40 M=1,NXP2
      IF(M.NE.1) GO TO 30
      W=(1.,0.)
      GO TO 35
   30 IP=IP+INC
      W=MULT(IP)
   35 CONTINUE
      DO 40 MXP=NXP,N,NXP
      J1=MXP-NXP+M
      J2=J1+NXP2
      T=X(J1)-X(J2)
      X(J1)=X(J1)+X(J2)
   40 X(J2)=W*T
      INC =INC+INC
   50 CONTINUE
      N2=N/2
      N1=N-1
      J=1
      DO 65 I=1,N1
      IF(I.GE.J) GO TO 55
      T=X(J)
      X(J)=X(I)
      X(I)=T
   55 K=N2
   60 IF(K.GE.J) GO TO 65
      J=J-K
      K=K/2
      GO TO 60
   65 J=J+K
```

```
      RETURN
      END


      SUBROUTINE WPOWER(W,N,INV)
      COMPLEX W(1),CMPLX
      W(1)=(1.,0.)
      PI=4.*ATAN(1.)
      ARG1=PI/FLOAT(N)
      SIGN=-1.
      IF(INV.EQ.1) SIGN=1.
      DO 10 I=2,N
      ARG2=ARG1*(I-1)
   10 W(I)=CMPLX(COS(ARG2),SIGN*SIN(ARG2))
      RETURN
      END
```

A FOURIER METHOD FOR IMAGE RECONSTRUCTION USING PROJECTION DATA

by

DAKSHESH D. PARIKH

B.E., M. S. University of Baroda, 1973

AN ABSTRACT OF A MASTER'S THESIS

submitted in partial fulfillment of the

requirements for the degree

MASTER OF SCIENCE

Department of Electrical Engineering

KANSAS STATE UNIVERSITY
Manhattan, Kansas

1976

The problem of reconstructing 3-dimensional objects from a set of 2-dimensional projected images is of great importance in fields ranging from medicine to radio astronomy. There has been a long-standing interest in this problem and a number of different techniques have been proposed. In this thesis, a 3N/2-Reconstruction Algorithm has been presented. The algorithm uses 3N/2 projection angles for an exact reconstruction of an (NxN) noiseless bandlimited digital image. Again, it is also shown that the exact reconstruction of an (NxN) digital image can be carried out using a single projection without resorting to any tedious computational techniques. Corresponding computer programs which enable one to generate projection data and reconstruct images via the 3N/2-Reconstruction Algorithm are also included.